

INFLUENCE OF DEPOSITION TEMPERATURE ON THE  
CORROSION RESISTANCE OF ELECTRODEPOSITED ZINC-  
NICKEL ALLOY COATINGS

**GOPI NATH NAMBIAR A/L MOHAN**

MECHANICAL ENGINEERING

UNIVERSITI TEKNOLOGI PETRONAS

JANUARY 2017

# **Influence of Deposition Temperature on the Corrosion Resistance of Electrodeposited Zinc-Nickel Alloy Coatings**

by

Gopi Nath Nambiar A/L Mohan

18290

Dissertation submitted in partial fulfillment of

as a Requirement for the

Bachelor of Engineering (Hons)

(Mechanical)

JANUARY 2017

Universiti Teknologi PETRONAS

Bandar Seri Iskandar

32610 Seri Iskandar

Perak Darul Ridzuan

Malaysia

CERTIFICATION OF APPROVAL

**Influence of Deposition Temperature on the Corrosion Resistance of  
Electrodeposited Zinc-Nickel Alloy Coatings**

by

Gopi Nath Nambiar A/L Mohan

18290

A project dissertation submitter to the

Mechanical Engineering Programme

Universiti Teknologi PETRONAS

In partial fulfilment of the requirement for the

BACHELOR OF ENGINEERING (Hons)

(MECHANICAL)

Approved by,

---

(Dr Saeid Kakooei)

UNIVERSITI TEKNOLOGI PETRONAS

BANDAR SERI ISKANDAR, PERAK

January 2017

## CERTIFICATION OF ORIGINALITY

This is to certify that I am responsible for the work submitted in this project, that the original work is my own except as specified in the references and acknowledgements, and that the original work contained herein have not been undertake or done by unspecified sources or persons.

---

GOPI NATH NAMBIAR A/L MOHAN

## ABSTRACT

Carbon steel, a metal used in various industrial applications as its functions and properties are apt and compatible with industrial functions are extremely prone to corrosion. Zinc and its alloys can be coated to provide corrosion protection to carbon steel and out of which, zinc-nickel alloy have been identified as the potential candidate as it possesses the highest corrosion resistance when compared with zinc in pure form. Deposition parameters play an important role in the microstructure, elemental composition and corrosion resistance property of zinc-nickel alloy. This paper focuses on the zinc-nickel alloy coatings which were electrodeposited on carbon steel from chloride bath using the technique of chronopotentiometry at different temperatures. The elemental composition and surface morphology analysis of zinc-nickel coated samples were done using SEM coupled with EDX. The coated samples were immersed in 3.5 wt% NaCl solution and measurements of corrosion resistance were done using LPR. SEM results shows that deposition temperature variation has a strong effect which changes the surface morphology and elemental composition of zinc-nickel alloy coatings. The nickel content in the electrodeposited zinc-nickel alloy coatings increases with increasing deposition temperature. Uniformity and compactness of coating decreases with increasing temperature. Cracks intensity increases with increasing deposition temperature which is attributed to internal stress due to factors might be related to hydrogen evolution reaction which causes hydrogen embrittlement. LPR results indicated that the coatings deposited at 25°C possessed the highest corrosion resistance after immersion in the 3.5 wt% NaCl solution for 24 hours. The LPR results correlate with the morphology and compositional properties of zinc-nickel alloy coatings deposited at different temperatures with decreasing corrosion resistance with increasing deposition temperature. Zinc-nickel alloy coatings with highest corrosion resistance, compact and dense morphology, better uniformity with less crack and nickel content within the range of 12 to 15% is achieved with zinc-nickel alloy coatings deposited at 25°C.

## **ACKNOWLEDGEMENTS**

I am very grateful for the opportunity given to undertake this project. Special appreciation goes to my supervisor, Dr. Saeid Kakooei for the endless support and guidance. I would like to convey my gratitude to him for the motivations and time spent up to completion of this project. My deepest appreciation and gratitude to Mr. Mohammadali Beheshti, graduate assistant who had provided guidance, support and a helping hand in conducting my project experimental work. My appreciation and gratitude also goes to the FYP I and FYP II coordinators, Dr. Turnad and Dr. Tamiru for assisting the students to the completion of the project. Besides that, my appreciation also goes to the staff and research assistants in Centre for Corrosion Research (CCR) for their continuous support for experiment conduct in CCR lab.

Finally, I would like to express my gigantic appreciation to my family members especially my father, Mohan and my beloved mother, Vimala for their unconditional love and supports. Lastly, thank you to my friends who support me through all these past 5 years in university. I am so thankful for our friendship and thank you for being the shoulder I can always depend on.

## **TABLE OF CONTENT**

<b>ABSTRACT .....</b>	<b>iv</b>
<b>ACKNOWLEDGEMENTS .....</b>	<b>vi</b>
<b>TABLE OF CONTENT.....</b>	<b>vi</b>
<b>LIST OF FIGURES .....</b>	<b>ix</b>
<b>LIST OF TABLES .....</b>	<b>xiv</b>
<b>ABBREVIATIONS.....</b>	<b>xv</b>
<b>CHAPTER 1: INTRODUCTION.....</b>	<b>1</b>
1.1 Project Background.....	1
1.2 Problem Statement .....	2
1.3 Objective .....	2
1.4 Scope of Study .....	2
<b>CHAPTER 2: LITERATURE REVIEW.....</b>	<b>5</b>
2.1 Carbon steel and its uses .....	5
2.2 Basics of Corrosion.....	5
2.3 Main Types of Corrosion .....	8
2.4 Methods of Corrosion Protection.....	9
2.4.1 Corrosion Resistant Surface Coatings.....	10
2.5 Basics of Electrodeposition .....	11
2.5.1 Zinc-Nickel Alloy Electrodeposition Technique ...	14
2.5.2 Anomalous type zinc-nickel alloy electrodeposition concept .....	14

2.6	Cadmium coatings .....	15
2.7	Zinc and its alloys as alternative to cadmium coatings ....	16
2.8	Zinc-nickel alloy corrosion behaviour .....	17
2.9	Factors affecting the corrosion behaviour of zinc-nickel alloy and optimization of these factors in relation to deposition temperature study .....	19
2.10	Electrochemical measurement technique.....	23
2.10.1	Linear Polarization Resistance (LPR).....	23
<b>CHAPTER 3: METHODOLOGY.....</b>		<b>25</b>
3.1	General FYP Flowchart .....	25
3.2	Project Methodology.....	27
3.2.1	Materials for Zinc-Nickel Alloy Electrodeposition	28
3.2.2	Chemicals for Electrodeposition of Zinc-Nickel Alloy.....	28
3.2.3	Preparation of Zinc-Nickel Bath Solution for Electrodeposition Process .....	28
3.2.4	Zinc-Nickel Alloy Electrodeposition Process.....	34
3.2.5	SEM Analysis .....	42
3.2.6	LPR Analysis .....	42
3.2.7	Corrosion rate and Compositional Reference Line (CRL) calculation.....	44
3.3	Key Milestones .....	46
3.4	Gantt Chart.....	47
<b>CHAPTER 4: RESULTS AND DISCUSSION .....</b>		<b>49</b>
4.1	Results and Discussion .....	49



4.1.1 Electrodeposition Process .....	49
4.1.2 Electrodeposited zinc-nickel alloy coatings.....	52
4.1.3 SEM and EDX Analysis .....	56
4.1.4 LPR Measurement.....	71
<b>CHAPTER 5: CONCLUSION AND RECOMMENDATION .....</b>	<b>78</b>
5.1 CONCLUSION.....	78
5.2 RECOMMENDATION .....	79
<b>REFERENCES.....</b>	<b>81</b>
<b>APPENDICES .....</b>	<b>86</b>

## LIST OF FIGURES

Figure 2.1	Illustration of electrodeposition process	12
Figure 2.2	Three-electrode electrochemical deposition schematic diagram	13
Figure 2.3	Metroehm Autolab obtained LPR Tafel plot (potential (V) vs. current (I))	24
Figure 3.1	General Flowchart for FYP Progress	25
Figure 3.2	Project Methodology	27
Figure 3.3	Heating using 'hot plate'	28
Figure 3.4	Zinc Chloride ( $\text{ZnCl}_2$ )	29
Figure 3.5	Weighing balance	29
Figure 3.6	Nickel Chloride Hexahydrate ( $\text{NiCl}_2 \cdot 6\text{H}_2\text{O}$ )	30
Figure 3.7	Ammonium Chloride ( $\text{NH}_4\text{Cl}$ )	31
Figure 3.8	Ammonia Solution 25%	32
Figure 3.9	Prepared 200mL Zinc-Nickel Alloy Bath Solution	33
Figure 3.10	Zinc-Nickel Alloy Solution in 250mL Scott Bottle	33
Figure 3.11	Mounted X52 low carbon steel	34
Figure 3.12	Grinder-Polisher Machine	34
Figure 3.13	Process of grinding	35
Figure 3.14	Sample Surface before grinding	35
Figure 3.15	Sample surface after grinding up to 1200 grit SiC paper	36

Figure 3.16	Polishing paper	37
Figure 3.17	Rough polishing (3 $\mu\text{m}$ polycrystalline diamond suspension)	37
Figure 3.18	Final polishing (1 $\mu\text{m}$ polycrystalline diamond suspension)	37
Figure 3.19	Polishing process in figure of eight manner	38
Figure 3.20	Mirror-like surface finish of sample after polishing process	38
Figure 3.21	Samples after polishing	38
Figure 3.22	Metroehm Autolab Potentiostat/Galvanostat with experimental setup for zinc-nickel alloy electrodeposition	40
Figure 3.23	Electrodeposition Setup for 25°C  (1) Pt mesh counter electrode, (2) Ag/AgCl reference electrode  (3) Epoxy mounted low carbon steel (working electrode),  (4) Zinc-Nickel Alloy Bath Solution	40
Figure 3.24	Setup for Electrodeposition at temperature 40°C, 60°C and 70°C	41
Figure 3.25	Electrodeposition Setup for 40°C, 60°C and 70°C  (1) Pt mesh counter electrode, (2) Ag/AgCl reference electrode  (3) Epoxy mounted low carbon steel (working electrode),  (4) Zinc-Nickel Alloy Bath Solution  (5) Thermometer (6) Magnetic Stirrer	41
Figure 3.26	Preparation of 3.5 wt% NaCl solution	42

Figure 3.27	Three-electrode electrochemical setup for LPR Analysis (1) Zn-Ni coated sample, (2) Stainless steel counter electrode (3) Ag/AgCl reference electrode, (4) 3.5 wt% NaCl solution	43
Figure 3.28	Metroehm Autolab Potentiostat/Galvanostat with experimental setup for LPR Analysis	43
Figure 4.1	Zinc-nickel deposition potential vs. time graph obtained at different temperatures of 25°C, 40°C, 60°C and 70°C	50
Figure 4.2	Zinc-nickel alloy coating formed for electrodeposition at 25°C	52
Figure 4.3	Zinc-nickel alloy coating formed at electrodeposition at 40°C	53
Figure 4.4	Zinc-nickel alloy coating formed for electrodeposition at 60°C	53
Figure 4.5	Zinc-nickel alloy coating formed for electrodeposition at 70°C	54
Figure 4.6	Images of coating formed at (a) 25°C and (b) 40°C	54
Figure 4.7	Images of coating formed at (a) 70°C and (b) 60°C	54
Figure 4.8	Images of coatings deposited at (a) 70°C, (b) 60°C, (c) 40°C and (d) 25°C	55
Figure 4.9	SEM images for electrodeposited zinc-nickel alloy coatings at (a) 25°C and (b) 40°C at magnification of 100x	56
Figure 4.10	SEM images for electrodeposited zinc-nickel alloy coatings at (a) 60°C and (b) 70°C at magnification of 100x	57

Figure 4.11	SEM image at 1000x magnification for zinc-nickel alloy coatings deposited at 25°C	58
Figure 4.12	SEM image at 2000x magnification for zinc-nickel alloy coatings deposited at 25°C	59
Figure 4.13	EDX Spectrum (a) and (b) for zinc-nickel alloy coatings deposited at 25°C	60
Figure 4.14	SEM image at 500x magnification for zinc-nickel alloy coatings deposited at 40°C	61
Figure 4.15	SEM image at 1000x magnification for zinc-nickel alloy coatings deposited at 40°C	61
Figure 4.16	EDX Spectrum for zinc-nickel alloy coatings deposited at 40°C	62
Figure 4.17	SEM image at 1000x magnification for zinc-nickel alloy coatings deposited at 60°C	63
Figure 4.18	SEM image at 3000x magnification for zinc-nickel alloy coatings deposited at 60°C	63
Figure 4.19	EDX Spectrum (a) and (b) for zinc-nickel alloy coatings deposited at 60°C	64
Figure 4.20	SEM image at 1000x magnification for zinc-nickel alloy coatings deposited at 70°C	65

Figure 4.21	SEM image at 3000x magnification for zinc-nickel alloy coatings deposited at 70°C	66
Figure 4.22	SEM image at 3000x magnification for zinc-nickel alloy coatings deposited at 70°C	66
Figure 4.23	EDX Spectrum (a) and (b) for observed microstructure for zinc-nickel alloy coatings deposited at 70°C	68
Figure 4.24	EDX Spectrum (a) and (b) for zinc-nickel alloy coatings deposited at 70°C	69
Figure 4.25	Zn-Ni content (wt%) vs Temperature (°C)	70
Figure 4.26	LPR corrosion rate measurements taken hourly for 24 hours	71
Figure 4.27	Average corrosion rate vs. zinc content	73
Figure 4.28	Average corrosion rate vs. nickel content	73
Figure 4.29	Observations on the coatings (a) 25°C (b) 40°C (c) 60°C and (d) 70°C after 24 hours immersion in 3.5 wt% NaCl solution	77

## LIST OF TABLES

Table 2.1	Summary of properties of various coatings with comparison to cadmium	17
Table 2.2	Corrosion current density/rate of different phase structured zinc-nickel alloy	18
Table 3.1	Electrodeposition parameters	39
Table 3.2	Key Milestone for FYP 1	46
Table 3.3	Key Milestone for FYP 2	46
Table 3.4	Gantt Chart for Timeline for FYP 1	47
Table 3.5	Gantt Chart for Timeline for FYP 2	48
Table 4.1	Average corrosion rate of samples coated and uncoated obtained using LPR method	72
Table 4.2	Relationship between deposition temperature and variation in properties of zinc-nickel alloy coatings obtained	76

## ABBREVIATIONS

Zn	Zinc
Ni	Nickel
Zn-Ni	Zinc-Nickel Alloy
Fe	Iron
Co	Cobalt
SEM	Scanning Electron Microscope
EDX	Energy Dispersive X-Ray Spectroscopy
LPR	Linear Polarization Resistance
NaCl	Sodium Chloride
Zn-Fe	Zinc-Iron Alloy
Zn-Co	Zinc-Cobalt Alloy
Sn-Zn	Tin-Zinc Alloy
Ni-Fe-P	Nickel-Iron-Phosphorus Alloy
Pt	Platinum
Ag/AgCl	Silver/Silver Chloride
$i_{\text{corr}}$	Corrosion current
$R_p$	Polarization Resistance
wt%	Weight percentage
mm/yr	millimetre per year



SiC	Silicon Carbide
Zn(OH <sub>2</sub> )	Zinc hydroxide
HER	Hydrogen Evolution Reaction
rpm	revolutions per minute

## **CHAPTER 1: INTRODUCTION**

### **1.1 Project Background**

Corrosion protection against steel are continuously being studied particularly on cathodic protection method. The metal currently being employed for protection of carbon steel are cadmium coatings, however these coatings provides environmental threat due to its toxicity. Studies are being extensively done to identify a possible alternative to the toxic cadmium coatings which poses minimal environmental threat as well as having sufficient or higher corrosion resistance ability as cadmium coatings.

Zinc is the common metal used for metal corrosion protection due to its high sacrificial property. Active metal corrosion resistance protection from highly corrosive surroundings is being widely studied especially on electrodeposited Zn and its alloys such as Co, Ni and Fe. When compared with combination of different Zn alloys, zinc-nickel alloy was found to be the best with highest corrosion resistance, thermal stability and great mechanical property.

For electrodeposited Zn–Ni alloy coatings, factors consisting of deposition parameters play a significant role in determining the formability, weldability and anti-corrosion performances in the electrodeposited alloy. Deposition parameter primarily consists of the bath composition, temperature, current density, deposition potential and bath pH. Variation in each parameter could lead to different types of alloy formation where changes could be observed in terms of its microstructure, composition and corrosion properties. Study focused on a specific deposition parameter on the electrodeposited alloy requires optimization of the other parameters at their optimum value while varying the specific deposition parameter that is being investigated.

Deposition temperature is one of the primary deposition parameter which influences the formation of alloy through electrodeposition process. The variations in the alloy formation at different temperatures can be investigated in terms of its structural and compositional properties and other physical properties such as micro hardness, internal stress, tensile strength, ductility, solderability and mainly corrosion resistance

behaviour. This project focuses on the study of the influence of deposition temperature on the corrosion behaviour of electrodeposited zinc-nickel alloy coatings.

## **1.2 Problem Statement**

An optimized electrodeposition process contributes heavily in the corrosion resistance behaviour of electrodeposited alloy. Deposition parameters play the most important role in the process of electrodeposition to form zinc-nickel alloy coatings. The electrodeposition of zinc-nickel alloy coatings is affected by many deposition parameter factors involving bath composition, temperature, current density, deposition potential and bath pH. Previous studies had been conducted on the effect of various deposition parameters on the microstructures and corrosion behavioural property of zinc-nickel alloy [1-7], however the parameter of the deposition temperature is not well explored in terms of corrosion resistance property and requires investigation as it directly influences the compositional and microstructural properties of zinc-nickel alloy coatings which in turn highly influences the corrosion resistance property of the alloy. Hence, the influence of deposition temperature have to be investigated through structural, elemental composition and corrosion resistance study in order to optimize the electrodeposition process to obtain the best surface and corrosion resistance properties of zinc-nickel alloy coatings.

## **1.3 Objectives**

The objectives of this project would be:

- a) To select the optimal electrodeposition parameters through literature review.
- b) To perform the zinc-nickel alloy electrodeposition process through varying the parameter of deposition temperature.
- c) To investigate the microstructural and elemental composition study on electrodeposited zinc-nickel alloy coatings.
- d) To determine the influence of various deposition temperature on the corrosion resistance of electrodeposited zinc-nickel alloy coatings.

## **1.4 Scope of Study**

The scope of study in this project will be primarily focused on experimental analysis of the electrodeposited zinc-nickel alloy with varying deposition temperature.

Scope of study in the electrodeposition part of zinc-nickel alloy starts with selection of the optimal deposition parameters through detailed study from past research papers on the electrodeposition process. Through optimization of these electrodeposition parameters, the required parameter to be tested on its influence on the corrosion behaviour of zinc-nickel alloy, the deposition temperature could be studied with better accuracy through experimental analysis. The deposition parameters to be made constant for each alloy deposition with varying deposition temperature are the bath composition, deposition potential, current density and bath pH.

The electrodeposition process is to be done with varying deposition temperature. The influence of the parameter to be tested, the deposition temperature is to be done in the following range of 25°C, 40°C, 60°C and 70°C within the range of ideal temperatures for alloy electrodeposition process which is between of 15°C to 70°C [8].

The electrodeposited zinc-nickel alloy coating will be analysed and studied in terms of:

a) Surface morphology and elemental composition

- i) Surface morphology and elemental composition analysis is done through the use of Scanning Electron Microscope (SEM).
- ii) Surface morphology analysis allows study of uniformity, stress and crack formation of the deposited alloy which influences corrosion behaviour of alloy using Scanning Electron Microscope (SEM) whereas the elemental composition of the alloy is studied using the SEM coupled with Energy Dispersive X-Ray Spectroscopy (EDX).

b) Corrosion behavioural analysis

- i) Immersion of electrodeposited zinc-nickel alloy coating into 3.5 wt% NaCl solution that simulates corrosive seawater environment and comparing corrosion readings recorded from Linear Polarization Resistance (LPR).
- ii) Linear Polarization Resistance (LPR) method measures the corrosion rate of alloy through for the zinc-nickel alloy in the corrosive

environment through constant observation of the relationship between the current from charged electrons and the electrochemical potential.

## **CHAPTER 2: LITERATURE REVIEW**

This chapter presents the gathered information and data on the project through literature review.

### **2.1 Carbon steel and its uses**

Carbon steel had been in use for most of the industrial applications such as for pipelines, automobile parts, marine applications, bolts and fasteners, aerospace industries involving aircraft gears and shafts, mining and construction. It has been regarded as the most widely used engineering material. However, a major concern that arises with the use of this carbon steel is its high corrosion rate with the common forms of corrosion attack being uniform, localized and galvanic.

### **2.2 Basics of Corrosion**

Corrosion is a characteristic natural process as it involves the conversion of a pure metal into a stable metal chemically in the form of oxides, sulfides and hydroxides. Slow deterioration of materials by chemical substance or electrochemical response with the environmental surroundings defines corrosion, in simple terms it is understandable as the electrochemical oxidation of metal when reacted with oxidant. The most widely recognised case of electrochemical corrosion is formation of iron oxides or commonly known as rust. This corrosion produces oxides or salts of the original metal in reddish-brown colouration. Valuable properties of materials and structures are deteriorated by corrosion process which affects the quality, appearance, strength and porousness to liquids and gases. Metals together with alloys undergoes corrosion through dampness or moisture exposure in air yet corrosion can also occur through exposure to certain corrosion inducing substances. Corrosion behaviour of metal is described depending on the material of the metal, stress and environment it is involved in.

The basics of corrosion is clearly explained with an electrochemical cell. Corrosion is an electrochemical process whereby electron transfer occurs between the anodic and

cathodic side. Presence of four components is needed to initiate corrosion which are the corrosion occurring site, anode which is, balanced by the cathode, the site at which no corrosion initiates, the electrolyte which is a current-conducting medium and a metallic or electrical connection presence flowing between the anode and cathode.

At the anode, corrosion or metal dissolution occurs and at the cathode, various cathodic reactions occur depending on nature and components of environment. Both the reactions are presented in equation (2.1), (2.2), (2.3) and (2.4).

Anode (oxidation):



Cathode (reduction)



In the case of corrosion of steel (iron), a droplet of water containing dissolved oxygen falls on the steel, the iron undergoes oxidation which is illustrated in equation (2.5).

Anode (oxidation):



The hydrogen ion in water ( $H_2O$ ) and dissolved oxygen,  $O_2(aq)$  grabs the electron at the droplet edge to produce water as described in equation (2.6):



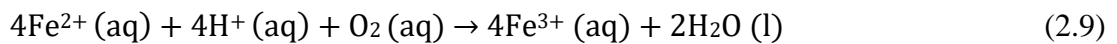
More acidic the water is, the higher the increase in corrosion. When the pH gets very low, the hydrogen ions will use the electrons due to high acidity taking over the cathodic reaction, making hydrogen gas as shown in equation (2.7):



The rust process utilizes hydrogen ions. pH of the droplet increase with the corrosion of iron. This results in the enhanced production of (OH<sup>-</sup>) hydroxide ions in water due to hydrogen concentration decrease. These OH<sup>-</sup> would then undergo reaction with Fe<sup>2+</sup> ions which produces insoluble iron(II) hydroxides as illustrated in equation (2.8):



Reaction of Fe<sup>2+</sup> ions with H<sup>+</sup> ions and O<sub>2</sub>(aq) also occurs at the same time to produce Fe<sup>3+</sup> ions as shown in equation (2.9):



The Fe<sup>3+</sup> ions would then involve in reaction with OH<sup>-</sup> ions eventually producing hydrated iron(III) oxides (commonly known as iron(III) hydroxide) as depicted in equation (2.10):



These Fe(OH)<sub>3</sub> then transforms gradually into Fe<sub>2</sub>O<sub>3</sub>•H<sub>2</sub>O (hydrated iron oxide) or commonly known as brown rust.

Corrosion are classified in many ways such as chemical and electrochemical corrosion, high and low temperature corrosion and wet and dry corrosion. Dry corrosion happens in the absence of aqueous environment with the presence of gases or vapors and at high temperatures. Wet corrosion involves aqueous environment which is focused in this project through immersion in NaCl solution.

There are various forms of corrosion and the main ones are discussed in the following chapter.



### **2.3 Main types of Corrosion**

There are different types and forms of corrosion identified and the common ones include general or uniform corrosion, localised corrosion, galvanic corrosion, concentration cell corrosion and microbially induced corrosion, erosion corrosion and stress corrosion cracking.

General corrosion is a form of corrosion attack which involves uniform attack over the entire exposed surface of material. It involves uniform loss of metal or material and the corrosion spreads over a large area of the surface. Localised corrosion involves corrosion attack on a confined small region of the metal and it takes the form of cavities. It is one of the most deteriorating type of corrosion and is found commonly on passive metals. Some of the localised corrosion types includes pitting and crevice corrosion. Galvanic corrosion occurs when dissimilar metals are exposed to the same electrolytic environment. The more noble metal corrodes the other, a less noble metal.

Concentration cell corrosion involves degradation of parts of metal at different rates as the parts come into contact with different concentrations of corrosive fluid or dissolved oxygen of the same electrolytic environment. It often occurs in presence of some physical barriers such as crevices and microbial mats. Microbially induced corrosion happens due to the presence of microorganisms of bacterial growth on the metal. Erosion corrosion involves corrosion attack in metal due to the mechanical action which involves relative motion of corrosive fluid and the surface of metal and stress corrosion cracking is due to cracking induced from the combined effect of tensile stress and corrosive environment.

Other forms of corrosion include selective leaching, intergranular and transgranular corrosion, fretting corrosion and high temperature corrosion. All these different types of corrosion are being continuously studied and explored to allow sustained and continuous improvement in the field of corrosion control. Corrosion control is extremely important as it involves the aspect of safety, environmental and cost. Various methods of corrosion protection are in study and also in practice in various fields involving corrosion.

## **2.4 Methods of Corrosion Protection**

Utilization of proper methods could manage, decrease and prevent metal corrosion. The efficiency of each technique is being continuously and extensively studied and improved. Identification of the type of corrosion prevention depends on the environment, mechanism and conditions involved in the metal corrosion. Six classification groups are identified for corrosion prevention which are modifications to the environment, selection of metal and conditions of surface, corrosion inhibitors, surface coating and cathodic protection.

Environmental modifications involve changing of process conditions which could eliminate or reduce corrosive species in the environment as the cause of corrosion is due to the reaction between metal and surrounding environment. Thus, by changing the surrounding environment or by removing the metal from the corrosive environment, corrosion can be substantially reduced.

Metal selection during design process plays a primary role in corrosion prevention. Understanding the environmental conditions involved allows proper selection of the metal to be used which eventually leads to corrosion reduction. Environmental conditions data can be correlated with the metal corrosion resistance data to choose the suitable metal with the highest corrosion resistance with respect to the environment. Not only that, surface condition monitoring and elimination of susceptible surface conditions also prevents corrosion.

Corrosion inhibitors are also commonly used in corrosion protection. Corrosion inhibitor chemicals react with the surface of metal and the corrosion inducing gas present in the environment thus intervening the chemically natural reaction which facilitate corrosion. Adsorption of inhibitors happen at the surface of metal hence a protection formation of film occurs. The application of inhibitors in the chemical form can be through insertion in solution and also applied in the form of protective coating which is achieved through dispersion method.

Cathodic protection is simply a technique used to control metal surface corrosion by making it the cathode of an electrochemical cell. The metal corrosion rate is generally reduced of a metallic structure through reduction of its corrosion potential the concept of shifting the metal nearer to the immune state.

Cathodic protection can be achieved by two widely used methods which are by coupling a given metal such as Fe with a more active metal such as zinc or magnesium. This produces a galvanic cell in which the active metal works as an anode and provides a flux of electrons to the metal, which then becomes the cathode. The cathode is protected and the anode progressively gets destroyed, and is hence, called a sacrificial anode.

The second method involves direct current application between the anode which is inert and protection required structure. The process involves electrons flowing to the structure where protection occurs by preventing the structure protected by becoming anode. The concept in applied current system involves the anode getting buried and application of low voltage DC current between the anode and the cathode.

#### **2.4.1 Corrosion resistant surface coatings**

Another excellent and common method of protecting the metal from corrosion will be through the use of surface coatings. The coatings applied could function as inhibitors, barrier or sacrificial. Coatings are classified into organic, non-organic, convertible and non-convertible. Some examples of corrosion protection coatings include sacrificial coatings such as galvanized steel, polymer coatings, ceramic coatings and corrosion or rust protection oils.

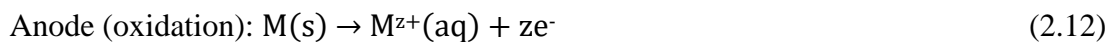
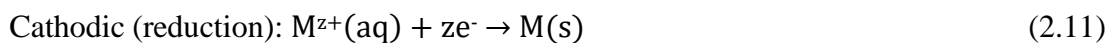
Current study utilizes this approach in the study of corrosion protection properties. Surface coatings on metals involves applying more noble metal which has greater corrosion resistance onto an active or less noble metal in the electrochemical series to protect the underlying metal from corrosion. Surface coatings can also be done alternatively by applying a more active metal to the metal to be protected which in this case the coating would corrode preferentially or sacrificially to the metal. The most common example of this type of protection is the galvanized steel where the active metal, zinc in the coating corrodes sacrificially and protects the steel. Various methods are employed in production of this surface coatings which are classified into vapor deposition method such as chemical vapor deposition and physical vapor deposition, spraying method such as spray painting, high velocity oxygen fuel, plasma and thermal spraying, roll-to-roll coating method such as gap coating, gravure coating and hot melt coating, dip coating method, spin coating method and electrochemical techniques such

as conversion coating, ion beam mixing, electroless deposition and **electrodeposition**, the coating method employed in current study to achieve surface coatings.

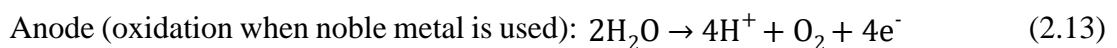
## 2.5 Basics of Electrodeposition

The process of electrodeposition basically utilizes electric current to facilitate the process of reduction of metal cations present in solution such that thin consistent metal coating is formed on the cathode surface. Application of electrodeposition involves changing and improving the surface and mechanical properties of a material like resistance towards wear, corrosion protection, achieving lubricant properties and qualities aesthetically. Besides that, electrodeposition application is also observed improving thickness on parts undersized and electroforming parts of materials.

The concept of electrodeposition as explained is related to a reversed relationship of a galvanic cell. Cathodic site constitutes the material which is to be deposited with the plating metal while the anode constitutes the metal that is to be used for deposition process to plate. Both metals are put in the bath or electrolyte solution consisting of the deposition metal salts and other ions to facilitate current flow. The current is applied inducing oxidation at the anode side releasing plating metal ions into the solution which eventually gets reduced at the surface of the cathode. This process is continuous as the bath solution containing the metal ions to be plated is continuously restored by the oxidation at anode. This process also termed as electrolysis in a summarized form is the forming of the anode metal at the cathode surface through reduction while the metal on the anode surface dissolves to restore the metals ions used up in the bath solution. The reaction at cathode and anode are shown in equation (2.11) and (2.12):



A noble metal such as platinum when used as anode in the process of electrodeposition, the reaction at anode changes into the process of oxidation of water as described in equation (2.13):



The use of more noble metal as anode will result in the anions undisturbed. This however results in the decrease in concentration of cations in the solution after each process of electrodeposition which requires replenishment and increase in  $H^+$  ions with time which might induce hydrogen evolution reaction.

A common example of electrodeposition is illustrated in Figure 2.1 for copper plating. Oxidation of copper happens in an acidic medium releasing electron forming  $Cu^{2+}$  ions. Association of  $Cu^{2+}$  ions with anions  $SO_4^{2-}$  ions happens in the solution forming copper sulfate. The cathodic side process involves  $Cu^{2+}$  ions getting reduced to metallic copper through obtaining two electrons released during oxidation process. This reaction phenomenon between cathode and anode causes copper transfer from anode to cathode surface.

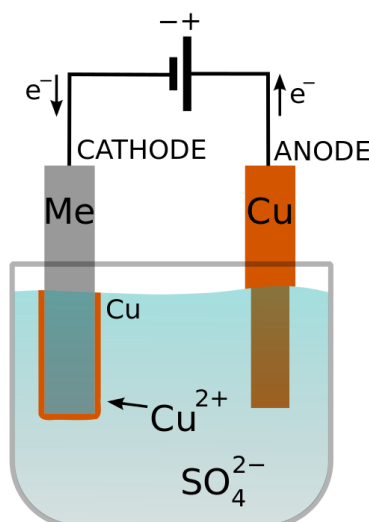


Figure 2.1: Illustration of Electrodeposition Process

Electrochemical deposition predominantly involves a three-electrode configuration whereby between the auxiliary and working electrodes a potential or current is applied. The working electrode potential is then measured with respect to the reference electrode. The base theory explaining electrochemical deposition experiments involves a oxidation-reduction or electron transfer reaction that must happen at the working electrode surface in order to facilitate the applied potential or current. Reduction of metal ions to metal occurs at the working electrode and this is balanced by a oxidation reaction which occurs at the counter or auxiliary electrode.

Electrochemical deposition involves electrochemical reaction which is a chemical reaction which happens at the interface between electrode and electrolyte of an electrochemical cell as a result of the transfer of electrons in between the electrolyte and the electrode, basically a redox, reduction-oxidation reaction where oxidation reaction occurs at anode and reduction reaction occurs at cathode. The concept is that electrochemical deposition is the process that uses reduction reactions to deposit the metal which is dissolved in the electrolyte as ions on the surface of the working electrode.

In this study, the method of electrochemical deposition is used to deposit zinc-nickel alloy coatings on metal electrodes. The three electrodes used are working, counter and reference electrodes respectively as shown in the Figure 2.2. The desired potential to supply electrons to the electrolyte during reduction reaction or transfer electrons from the electrolyte during oxidation reaction is applied at the working electrode. The reference electrode has a defined potential and functions to measure the potential of the working electrode and it should not pass any current through it. Counter electrode functions to maintain the current flow. The surface area of the counter electrode is generally is made larger than that of the working electrode in order to keep a uniform current flow through the working electrode.

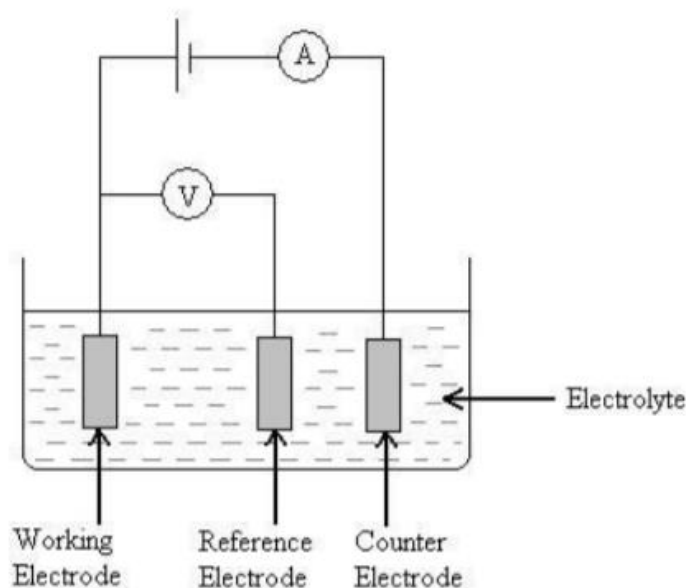


Figure 2.2: Three-electrode electrochemical deposition schematic diagram

There are various methods of electrochemical deposition which are classified into potentiometry, voltammetry, and coulometry which are discussed in the following section.

### **2.5.1 Zinc-nickel alloy electrodeposition technique**

Various methods can be used to perform electrodeposition electrochemically namely potentiometry consisting of methods like chronopotentiometry, coulometry consisting of methods like potentiostatic coulometry and voltammetry consisting of methods like polarography and chronoamperometry. The electrodeposition methods are chosen through experiments, by comparing analytical results obtained such as corrosion measurements and coating microstructural study with different electrodeposition technique employed. In this project, the technique of chronopotentiometry was used to carry out electrodeposition to obtain zinc-nickel alloy coatings. The chronopotentiometry method is a galvanostatic method wherein a constant current is applied and the resulting potential is measured over time. A research conducted compared the zinc-nickel alloy coatings obtained through electrodeposition techniques of chronopotentiometry and cyclic voltammetry [9]. The results obtained through microstructural studies revealed a more compact surface morphology of fine grain size with higher coating thickness and better composition of zinc-nickel in the coatings, whereas the results from corrosion measurements of electrochemical impedance spectroscopy and potentiodynamic polarization showed higher corrosion resistance for coatings deposited under chronopotentiometry method. The research was concluded providing data on the suitability of the method chronopotentiometry on electrodeposition of zinc-nickel alloy. This chronopotentiometry method was chosen for electrodeposition for this project due to the suitability of this method when compared to other methods for electrodeposition.

### **2.5.2 Anomalous type zinc-nickel alloy electrodeposition concept**

The electrodeposition of zinc-nickel alloy can be related to both anomalous and normal type. The normal alloy electrodeposition process generally involves the more noble metal being deposited preferentially due to greater driving force of the more noble metal to be deposited. However, in the electrodeposition of iron-group metals with an active metal, Zn, anomalous type deposition is observed.

Cathodic deposition half reactions of both Zn and Ni are presented in equations (2.14) and (2.15):



The less noble or active metal, zinc is preferentially deposited on the alloy when compared to the more noble metal, nickel. Anomalous co-deposition is the preferential deposition of the less noble metal when compared to more noble metal and the percentage of the less noble metal in the deposit is higher than that of the metal salt present in the bath solution. In the case of zinc-nickel, the percentage of zinc in the deposit is higher than that of its salt in the electrolyte.

This anomalous phenomenon is observed only in certain alloy electrodeposition namely iron-group metals with less noble zinc, cadmium and manganese. Many theories have been proposed to the occurrence of this mechanism of anomalous co-deposition and the most widely accepted theory is the hydroxide suppression mechanism [10]. Based on this theory, the deposition of more noble metal, nickel is suppressed in the presence of zinc hydroxide,  $\text{Zn}(\text{OH}_2)$  preferentially formed and absorbed on the cathode. Zinc reacts with hydroxide ions forming  $\text{Zn}(\text{OH}_2)$  which becomes more noble than nickel resulting in preferred deposition of zinc and nickel deposition getting suppressed by these zinc hydroxide formations.

The zinc-nickel alloy deposition process is influenced by various electrodeposition factors consisting of temperature, current density, bath pH and composition and deposition potential and the preferred zinc-nickel composition (12 to 15 wt% nickel) falls under the anomalous type which can be achieved through variation and control of these deposition factors [11].

## 2.6 Cadmium coatings

Electrodeposited cadmium has been a primary choice for steel surface protection for many years due to its high corrosion resistance property being able to provide cathodic protection to steel. Cadmium coatings have been previously used in the aerospace, mining, automotive, defence and oil and gas industries where their application are towards bolts and other fasteners, chassis, connectors and other components. The



utilization of cadmium is however under scrutiny because of its lethal nature and ecological risk. Zinc and its alloy had been identified as a potential replacement for cadmium coatings.

## **2.7 Zinc and its alloy as alternatives to cadmium coatings**

Zinc electroplating as an another option to cadmium has been examined for its corrosion protection abilities due to its sacrificial property and has proved its ability by providing satisfactory corrosion behaviour results through study done on the corrosion resistance and mechanical properties of electrodeposition of zinc [12]. Although zinc is looked as a possible alternative, its corrosion behaviour doesn't look really good on aggressive environment, higher temperature conditions. Evidence from the study on the electrodeposited zinc coatings mentioned pure zinc having poor corrosion resistance properties than that of cadmium [13]. Hence, the necessities for metallic coatings with corrosion resistance superior to that of pure zinc and of comparability or superior than cadmium have prompted to the industrial generation of electrodeposits in regards of zinc alloys with group eight metals, for example, Zn-Ni, Zn-Co, Zn-Fe [14]. Electrodeposition of Zn and its metals of eight group such as Fe, Co and Ni are widely being studied and analysed due to its capability of being of excellent corrosion resistant alloy. Table 2.1 extracted mentions that involving all Zn combinations of alloys, Zn-Ni alloy coatings have pulled in more interest because of its equivalence with the cadmium properties [13].

Table 2.1: Summary of properties of various coatings with comparison to cadmium

Coating	Corrosion resistance	Sacrificial protection	Formation of voluminous corrosion products	Uniform deposition	Adhesion
Electrodeposited cadmium	good	good	low	good	good
Electrodeposited Zn-Ni	good	good	low	good	good
Electrodeposited Zinc	poor	good	high	good	good
Electrodeposited Sn-Zn	good	good	low	good	good
Electrodeposited Zn-Co	fair	good	intermediate	good	good

## 2.8 Zinc-nickel alloy corrosion behaviour

Many researches have been conducted in the past years to analyse the possibilities of zinc-nickel alloy being a replacement with corrosion resistance property equivalent to toxic cadmium coatings. Many previous researches have also been conducted to identify and measure the corrosion resistance ability of zinc-nickel alloy [3, 14-21]. Corrosion resistance of zinc-nickel alloy deposited on high strength steel mentioned the best corrosion resistance property is achieved for zinc-nickel alloy in the range of 12 to 15 wt% of nickel content in the alloy whereby the alloy with nickel content (12 to 15%) retains the anodic behaviour to steel, maintaining sacrificial protection but with a lower corrosion rate as a result of nickel addition raising the potential closer to steel providing corrosion protection for longer period of time [14]. This is further supported by studies done by other authors [3, 15, 16] who mentioned that zinc-nickel alloy with nickel content in the range of 12 to 15 wt% provides excellent corrosion resistance where the alloy maintains its sacrificial behaviour with respect to steel substrate whereas alloy beyond 30 wt% of nickel becomes more noble than the steel

substrate losing its sacrificial property which leads to steel being corroded preferentially and nickel content of below 10 wt% in the alloy results in lower barrier properties. Not only that, another research provides evidence from Table 2.2 of the best corrosion resistance properties using weak acid chloride bath being Zn-15%Ni alloy having the lowest corrosion current density indicative of highest corrosion resistance and this is attributed to the presence of  $\gamma$ -phase ( $\text{Ni}_5\text{Zn}_{21}$ ) which is obtained with zinc-nickel alloys of 12 to 15 wt% nickel content [21]. Zinc-nickel alloy coatings with 10–15 wt.% of Ni have better corrosion resistance, superior formability and improved weldability [18]. Presence of nickel in the zinc-nickel alloy at the optimum range of 12 to 15% slows down the rate of dissolution of zinc, providing higher and prolonged corrosion resistance than pure zinc.

Table 2.2: Corrosion current density/rate of different phase structured zinc-nickel alloy

<b>Effect of chemical and phase composition on corrosion resistance of zinc-nickel alloy coatings</b>			
<b>Plating bath</b>	<b>Ni, wt. %</b>	<b>Phase composition</b>	<b>Corrosion current density, <math>\mu\text{A cm}^{-2}</math></b>
Weak acid chloride	15.0	$\gamma$ -phase	Lowest
	20.7	$\gamma$ -phase + polycrystalline Ni	2.0-2.5
	25.2 – 28.0	Solid solution of Ni in $\gamma$ -phase + polycrystalline Ni	High
	66.0	$\alpha$ -phase	Highest

These studies focused on the influence of specific alloy metal on the corrosion behaviour of alloy, in this case the influence of nickel on corrosion behaviour of zinc-nickel alloy. An alloy electrodeposition process as well as deposition parameter factors also affect corrosion resistance property such as bath composition, temperature, bath agitation, current density, deposition potential and bath pH.

## **2.9 Factors affecting the corrosion behaviour of zinc-nickel alloy and optimization of these factors in relation to deposition temperature study**

Previous researches have conducted many experiments on the influence of these factors or parameters on the alloy electrodeposition process and corrosion behavioural property. Many researches have focused on the effects of different electrodeposition parameters on the electrodeposition process of different types of alloys studying their phase structures, composition, surface morphological properties and the corrosion behavioural property to reveal their influences [1-7]. Study focusing on effect of a specific deposition parameter which in this case is the deposition temperature requires other deposition parameters consisting of bath pH and composition, current density and bath agitation to be held at a constant optimum value. Selection of these parameters at their optimized value was done through literature review study focusing on the effect of these parameters towards the electrodeposition and corrosion behaviour of the alloy.

Based on the findings from literature review study in an effort to optimize the deposition parameters, studies focusing on the effects of the bath pH on the alloy electrodeposition process has shown that the bath pH has significant effect on the hydrogen evolution reaction (HER) and also the surface morphology and quality of the alloy coatings deposited. HER is the production of hydrogen through the process of water electrolysis. This hydrogen produced would then diffuse into the coatings during the process of electrodeposition causing rise in internal stress and brittleness inducing defects in the form of cracks in the coatings. It is important to minimize the facilitation of this HER reaction through proper optimization of the parameters.

At a very low pH of 1, the surface morphology of the coatings obtained were rough, non-homogeneous and non-uniform. The electrodeposition process was also highly susceptible to HER. This is due to the acidity of the bath at low pH. However, with increasing pH, the uniformity and homogeneity of the coatings improves with susceptibility to hydrogen evolution reaction still high and with further increase in pH up to 5, quality, uniformity and homogeneity of coatings improves further with reduced susceptibility to HER causing hydrogen embrittlement. Hence, higher pH with decreasing acidity approaching the state of neutrality is preferred for the alloy

electrodeposition process due to decrease in hydrogen evolution and better surface morphology deposited [22, 23].

Zinc-nickel bath composition related studies revealed effects towards the type of alloy deposition that predominantly occurs with variation in the composition of zinc and nickel in the bath solution. At a low bath composition with Zn(II)/Ni(II) molar ratio between 0.25 to 1, normal co-deposition of alloy is achieved. This is due to the higher concentration of nickel in the bath resulting in higher deposition of nickel of more than 40% in the coatings. The cathodic efficiency and deposition rate is also observed to be low of less than 60% at lower Zn(II)/Ni(II) molar ratio in the bath. For Zn(II)/Ni(II) molar ratio between 1 to 2 in the bath solution, anomalous type of alloy deposition is achieved which results in higher amount of zinc getting deposited in the coatings. This range of bath composition is also found to be conducive to obtain coatings with lower nickel content between 12% to 15%, the ideal composition for increased corrosion resistance. High deposition rate and cathodic efficiency of more than 95% is also achieved for this range of zinc-nickel molar ratio. Further increase in the Zn(II)/Ni(II) molar ratio to the range of 2 to 4 in the bath solution, anomalous type of alloy deposition is observed however the nickel content in the deposited coatings seem to be too low of less than 5%. This is due to the extremely high concentration of zinc when compared to nickel in the bath solution, leading to very low nickel deposition in the coatings. Similar observation of high deposition rate and cathodic efficiency of more than 95% of that of Zn(II)/Ni(II) molar ratio in the range of 1 to 2 is also achieved in this range of Zn(II)/Ni(II) molar ratio. Zn(II)/Ni(II) molar ratio of between 1 to 2 was found to be favourable in achieving anomalous type of alloy electrodeposition with the nickel content ranging in the required value of 12% to 15% with high cathodic efficiency and deposition rate [21, 24, 25] .

Studies on the effect of bath agitation towards the alloy electrodeposition process revealed that bath agitation has impact towards the uniformity of the coatings obtained where at a lower range of agitation at 100 rpm, the quality of deposit obtained is non-uniform because of low rate of ion transportation to the cathode surface. The agitation rate is insufficient to support the applied current of 10 mA/cm<sup>2</sup> at the cathode surface, however with increase in agitation to 300 rpm, uniform and adherent coatings were produced at the current density of 10 mA/cm<sup>2</sup>. The rate of ion consumption at the

cathode surface matches the ion transport at this agitation and smooth flow of ions to the cathode surface is achieved at 300 rpm. Further increase in bath agitation up to 600 rpm results in the deposited coatings formed to be powdery. This is related to the high turbulence at higher rate of agitation and higher rate of ion transported to the cathode surface and the applied current of 10 mA/cm<sup>2</sup> not being able to support the ion transport to ion consumption. Higher current density of more than 50 mA/cm<sup>2</sup> is required to achieve a uniform and homogeneous deposit at this higher rate of bath agitation of 600 rpm. Intermediate bath agitation rate of 300 rpm was observed to be ideal to obtain quality coatings of good uniformity [26, 27].

The effect of current density towards the alloy electrodeposition process was observed to be more of its role in determining which metal is facilitated in the deposition of zinc-nickel alloy coatings at different current densities. At low current density of 10 mA/cm<sup>2</sup>, the deposition of zinc is more facilitated in the coating. The activity of nickel is suppressed by zinc at low current density resulting in mass discharge of zinc at the cathode surface and decrease in nickel deposition. This is related to hydroxide suppression mechanism of anomalous deposition and is required to achieve coatings with high zinc content of more than 80 wt% to maintain the corrosion resistant properties of zinc-nickel alloy. Further increase of current density to 50 mA/cm<sup>2</sup> leads to decrease in the consumption rate of zinc ions on the cathode surface which is due to the decrease in facilitation of zinc hydroxide formation. This results in lower rate of zinc hydroxide formation which is the primary factor which facilitates zinc deposition in the coating and hence the driving force or activity for the deposition of nickel and hydrogen increases which results in increased facilitation of nickel and hydrogen deposit in the coatings at higher current density of 50 mA/cm<sup>2</sup>. Very high current densities up to 100 mA/cm<sup>2</sup>, the deposition of nickel is facilitated in preference to hydrogen and zinc, resulting in higher nickel content in the coatings and very low zinc content. Observations from current density effect study towards the alloy electrodeposition process revealed low current density (10 mA/cm<sup>2</sup>) facilitating the preferred zinc deposition and higher current densities (50 and 100 mA/cm<sup>2</sup>) facilitating nickel and hydrogen deposition leading to higher nickel content and hydrogen embrittlement issue [21, 27-29].

Optimization of these deposition parameters described above were done through literature review study to allow study of deposition temperature parameter experimentally. Selection of other parameters at the optimum value enhances and better validate the results obtained on study focusing on specific deposition parameter which in this case is the deposition temperature.

Deposition temperature is one of the important parameter that impacts the electrodeposition process as well as the corrosion resistance property of alloy. Variation in temperature has significant effect towards the electrodeposition process, which results in change in microstructural and elemental compositional property which in turn is reflected in the corrosion behaviour of the alloy. Previous researches had been done on the influence of deposition temperature on alloy electrodeposition such as a study done on the effects of temperature on the electrodeposition of Ni-Fe-P alloy where results of influence of variation of temperature on the structural and surface morphological properties of the alloy were analysed and studied [4]. Adverse changes were observed in the microstructure and composition of alloy when the temperature is varied [4]. However, not many researches have been conducted on the influence of temperature on zinc-nickel alloy especially on its corrosion resistance. A research conducted on the deposition temperature studied the effect of deposition temperature on electrodeposited zinc-nickel alloy coatings focusing on the surface morphology, phase structure and alloy composition properties of the deposited coatings at different temperatures [30]. Observations from this study mentioned on the increasing nickel content and deterioration of surface properties of zinc-nickel alloy coatings with increasing temperature, however no further analysis were done on the corrosion resistance properties of the alloy under different deposition temperature and the relationship between the temperature and surface morphology, phase and alloy composition obtained through this study were not explored in terms of its effect on the corrosion resistance of zinc-nickel alloy coatings.

In this present study, the influence of various deposition temperature focusing on the corrosion resistance of electrodeposited zinc-nickel alloy using chloride bath is to be determined. This is to be done by conducting the corrosion behavioural study in terms of Linear Polarization Resistance (LPR) technique and surface morphology characterization study through Scanning Electron Microscope (SEM) technique.

Based on the experimental analysis on the influence of various deposition temperature on the corrosion behaviour, the deposition temperature which provides the highest corrosion resistance is to be identified. The technique employed for electrodeposition of zinc-nickel alloy coatings is chronopotentiometry.

## 2.10 Electrochemical measurement technique

In this present study, the influence of deposition temperature on the corrosion resistance of electrodeposited zinc-nickel alloy coatings are analysed using LPR technique. Electrochemical tests have been identified to be one of the two methods used in experimental determination of corrosion rate, the other being immersion or weight loss test. LPR is known to provide accurate and better results of corrosion rate. Both these electrochemical corrosion measurement techniques were employed in this project and measurements of corrosion rate were done based on standards designed to these techniques.

### 2.10.1 Linear Polarization Resistance (LPR)

Linear Polarization Resistance method allows measurement of corrosion rate in real time. The system's polarization resistance,  $R_p$  is measured through the slope of Tafel plot and the corrosion rate is calculated through formulas from the standards given.

The general procedure for LPR measurement is briefly explained. Voltage sweep of -/+ 10mV is applied across the working and reference electrode. The resulting current response is measured. The measurements are done by measuring the Tafel plot consisting of potential ( $E$ ) vs. current density ( $i_{corr}$ ) about the free corrosion potential ( $E_{corr}$ ). Polarisation resistance ( $R_p$ ) is measured from the slope of potential( $E$ ) vs current density ( $i_{corr}$ ) plot.  $R_p$  ( $\Omega\text{cm}^2$ ) from measurement is then used calculate the corrosion rate using Stern & Geary equations. The corrosion rate in oilfield units of mm/yr can then be calculated. Stern-Geary theory clearly illustrates this LPR concept:

$$R_p = \frac{\Delta E}{\Delta I} = \frac{\beta_a \beta_c}{2.3 \cdot i_{corr} \cdot (\beta_a + \beta_c)} \quad (2.16)$$

where  $\beta_a$  and  $\beta_c$  represents the anodic and cathodic reactions Tafel slopes.



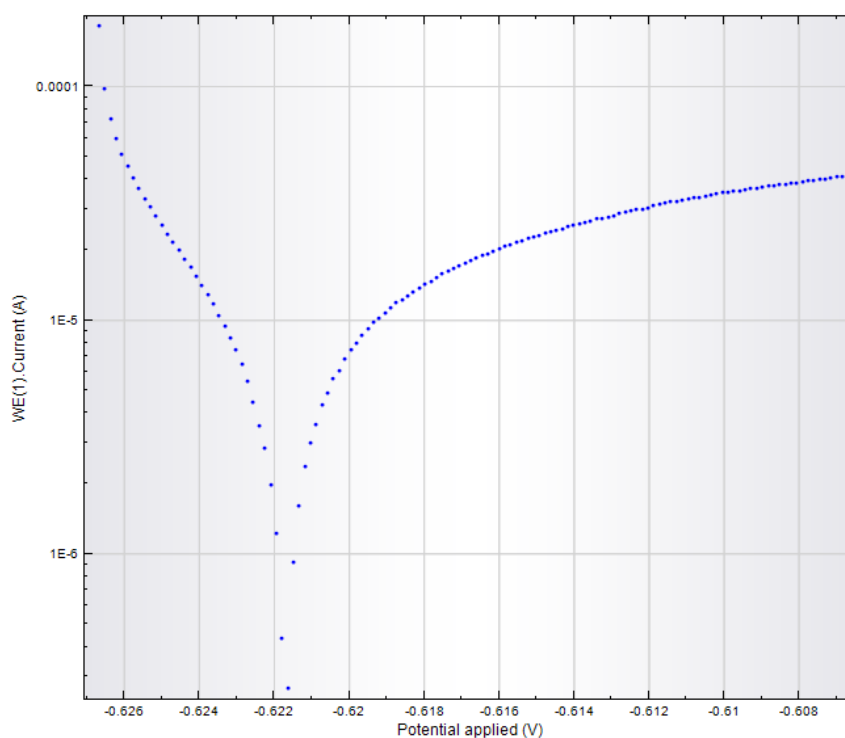


Figure 2.3: Metrohm Autolab obtained LPR Tafel plot (potential (V) vs. current (I))

The advantages of LPR is that it is relatively easy to set-up, non-destructive to electrode surface, able to run repeatedly to monitor corrosion rate over time, good for screening a range of inhibitors and determining approximate dose rates. However, LPR only measures general corrosion.

## CHAPTER 3: METHODOLOGY/PROJECT WORK

### 3.1 General FYP Flowchart

Flowchart below highlights the general flow or progress of Final Year Project:

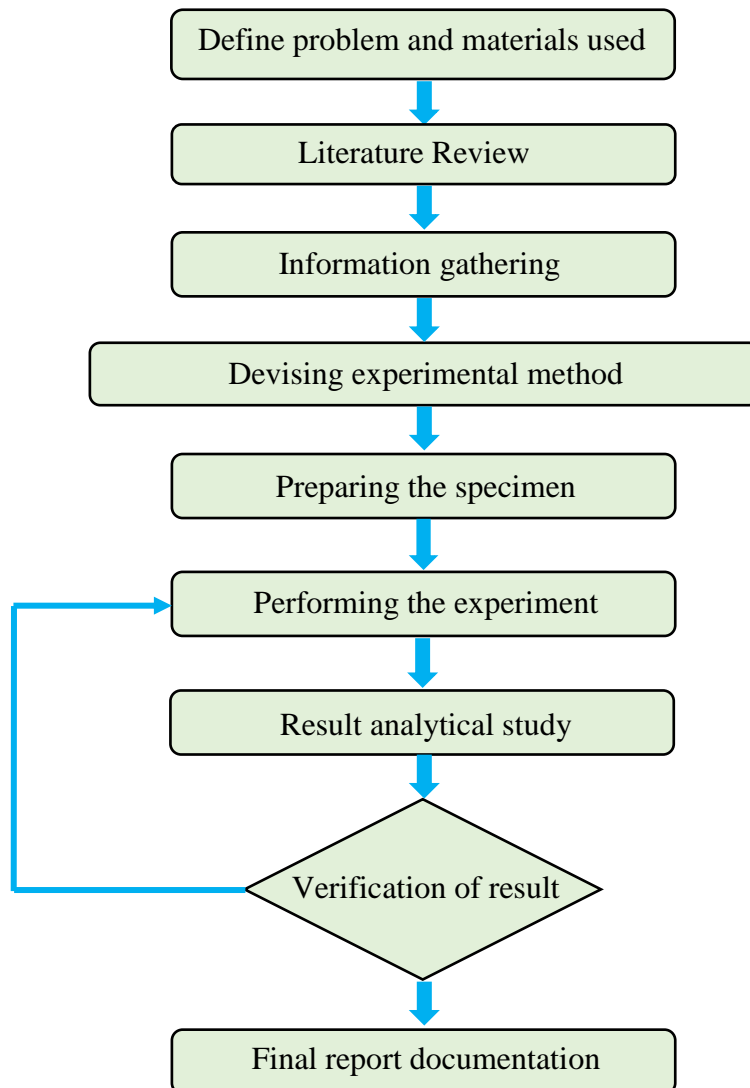
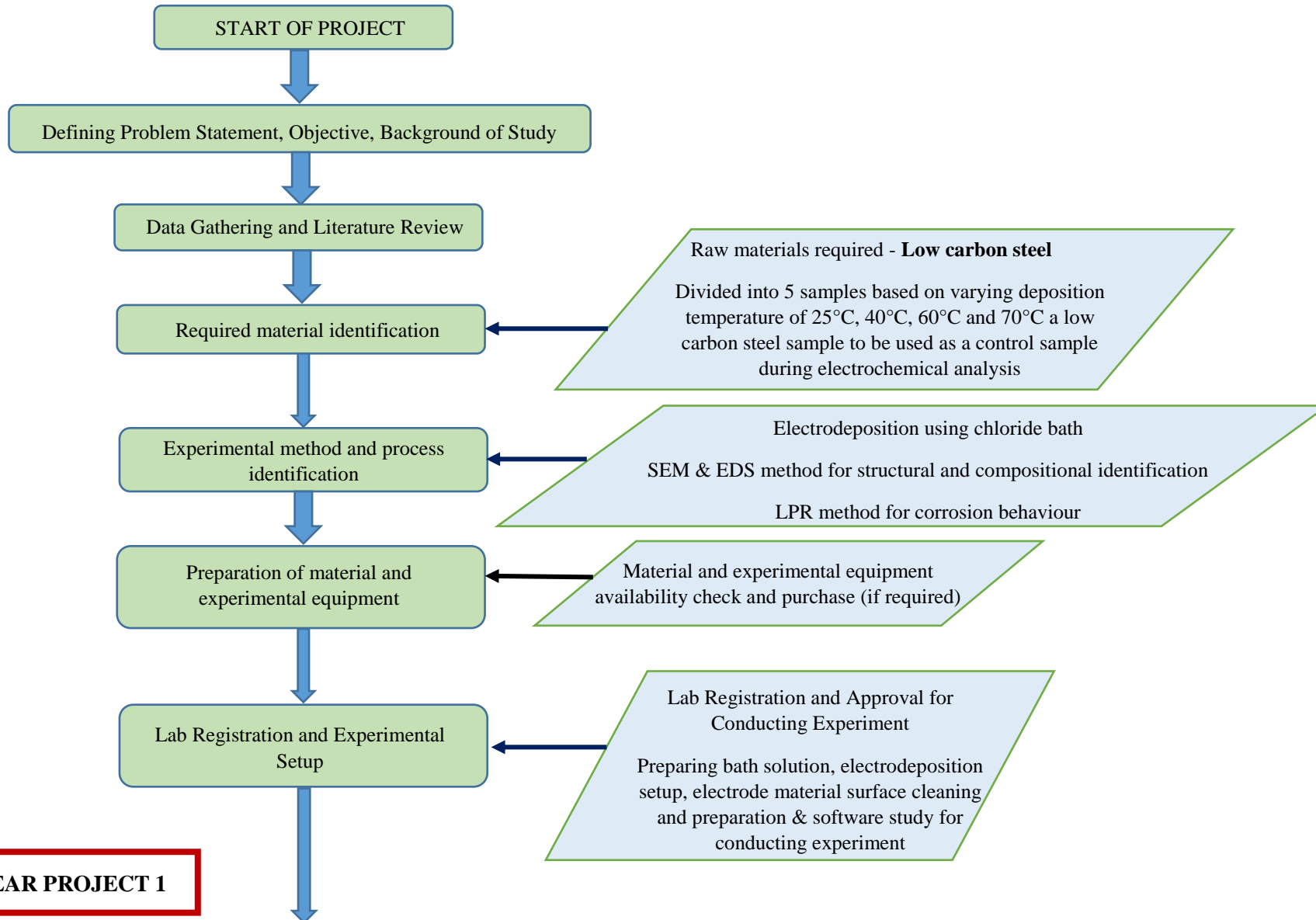


Figure 3.1: General Flowchart for FYP Progress

### 3.2 Project Methodology



## FINAL YEAR PROJECT 2

Conducting the experiment

Experiment Result Analysis and Documentation

Project Presentation

Analysis of results obtained from SEM, LPR technique  
Final project report preparation & submission

### Electrodeposition of Zinc-Nickel Alloy:

Working electrode: Low carbon steel

Auxiliary electrode: Platinum mesh

Reference electrode: Ag/AgCl

Bath composition: Chloride bath

ZnCl<sub>2</sub>, NiCl<sub>2</sub>, NH<sub>4</sub>Cl

### Parameter to be varied:

Deposition temperature (25°C, 40°C, 60°C and 70°C)

### Parameter to be controlled at constant rate:

Current density, pH, plating time and bath composition.

### Corrosion behavioural analysis:

LPR technique

3 electrode cell setup

Working electrode: Electrodeposited zinc-nickel alloy

Auxiliary electrode: Platinum mesh electrode

Reference electrode: Ag/AgCl

Bath solution: 3.5% NaCl solution

Figure 3.2: Project Methodology

### 3.2.1 Materials for Zinc-Nickel Alloy Electrodeposition

The carbon steel that is used for this project is API 5L X52 low carbon steel. The X52 carbon steel is cut into 5 samples to be deposited with zinc-nickel alloy coatings at 25°C, 40°C, 60°C and 70°C and a control sample for comparison analysis during electrochemical test.

### 3.2.2 Chemicals for Electrodeposition of Zinc-Nickel Alloy

Zinc (II) chloride ( $\text{ZnCl}_2$ ), Nickel (II) chloride hexahydrate ( $\text{NiCl}_2 \cdot 6\text{H}_2\text{O}$ ), Ammonium chloride ( $\text{NH}_4\text{Cl}$ ) were used for alloy bath preparation and Ammonia solution 25% to adjust pH of bath solution. All solution were prepared using distilled water [30].

### 3.2.3 Preparation of Zn-Ni Bath Solution for Electrodeposition Process

The Zinc-Nickel Alloy Solution was prepared in the laboratory with reference to [30] on optimized bath composition to allow study on the parameter of deposition temperature to be conducted. Following are the order of solution preparation:

1. 200mL of distilled water was weighed using a weighing balance and added to 500mL glass beaker. (Density of distilled water =  $1 \text{ g/cm}^3$ , 200ml =  $200 \text{ g/cm}^3$ )
2. The beaker containing distilled water was heated using hot plate to the range of 45 to 60 °C as illustrated in Figure 3.3.



Figure 3.3: Heating using 'hot plate'

3. The required quantity of 16 g of  $\text{ZnCl}_2$  was measured and weighed using the weighing balance. Figure 3.4 and Figure 3.5 illustrates the procedure.

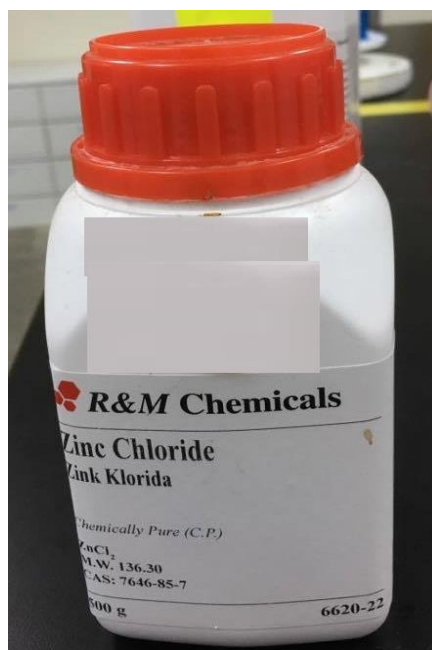


Figure 3.4: Zinc Chloride ( $\text{ZnCl}_2$ )



Figure 3.5: Weighing balance

4. 16 g of  $\text{ZnCl}_2$  was then added to the 200mL distilled water. Water temperature during addition of  $\text{ZnCl}_2$  was recorded to be at 30 °C. (Temperature adjusted in hot plate = 60 °C and the magnetic stirring speed is set at 700 rpm.)
5. The mixture of solution was stirred for 10 minutes to dissolve completely.

6. The required quantity of 22 g of  $\text{NiCl}_2 \cdot 6\text{H}_2\text{O}$  was measured and weighed using the weighing balance. Figure 3.6 illustrates the  $\text{NiCl}_2 \cdot 6\text{H}_2\text{O}$  chemical container.



Figure 3.6: Nickel Chloride Hexahydrate ( $\text{NiCl}_2 \cdot 6\text{H}_2\text{O}$ )

7. 22 g of  $\text{NiCl}_2 \cdot 6\text{H}_2\text{O}$  was then added to the 200mL distilled water. Water temperature during addition of  $\text{NiCl}_2 \cdot 6\text{H}_2\text{O}$  was recorded to be at 37.5 °C. (Temperature adjusted in hot plate = 85 °C, the temperature is set higher than the required temperature at the hot plate to accommodate the excessive heat loss to the surroundings during heating of the solution and the magnetic stirring speed is set at 700 rpm.)
8. The mixture of solution was stirred for 10 minutes to dissolve completely. The solution was observed to turn 'green' once the  $\text{NiCl}_2 \cdot 6\text{H}_2\text{O}$  starts to dissolve with respect to the colour of  $\text{NiCl}_2 \cdot 6\text{H}_2\text{O}$  in solid state in the form of green crystals.
9. The required quantity of 44 g of  $\text{NH}_4\text{Cl}$  was measured and weighed using the weighing balance. Figure 3.7 depicts the  $\text{NH}_4\text{Cl}$  chemical container.

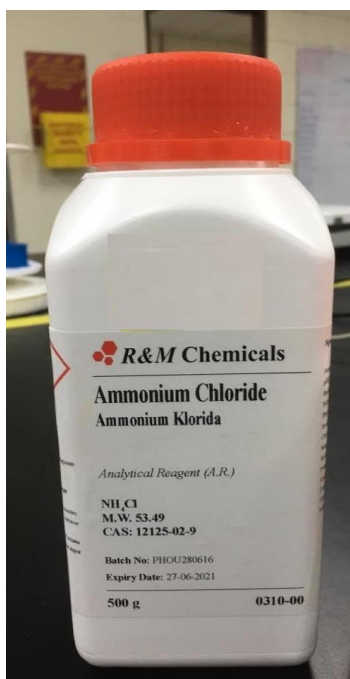


Figure 3.7: Ammonium Chloride (NH<sub>4</sub>Cl)

10. 44 g of NH<sub>4</sub>Cl was then added to the 200mL distilled water. Water temperature during addition of NH<sub>4</sub>Cl was recorded to be at 45 °C. (Hot plate temperature control switch is turned off to allow solution temperature to cool down and the magnetic stirring speed is set at 700 rpm.)
11. The mixture of solution was stirred for 10 minutes to dissolve completely.
12. The temperature of solution was measured using thermometer at 28 °C.
13. The pH of solution was measured using a pH meter at pH 4.13 before adding ammonia.
14. Ammonia solution 25% as shown in Figure 3.8 was added to the solution to increase the pH of solution to the required level of pH 5.



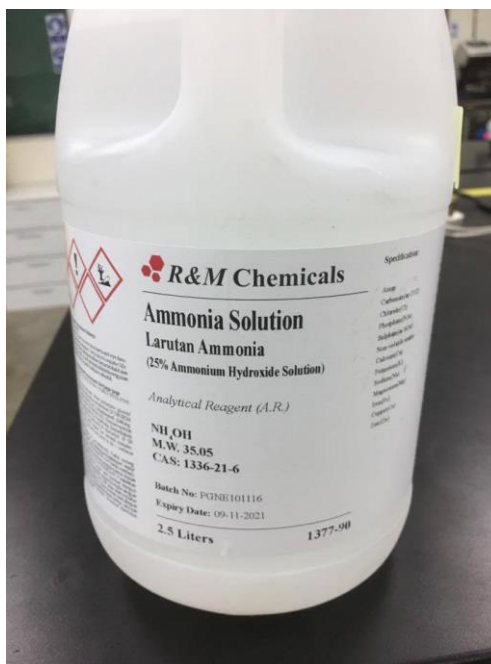


Figure 3.8: Ammonia Solution 25%

15. 10mL of ammonia solution 25% was poured into a 100mL beaker and a dropper was used to take in required quantity to be added into the solution.
16. 1.25mL of ammonia was first added into the solution using the dropper.
17. The solution was stirred using glass rod and the pH reading was taken using pH meter. The pH was recorded to be at pH 4.90.
18. An additional amount of 0.25mL of ammonia was then added into the solution using the dropper.
19. The solution was stirred using glass rod and the pH reading was taken using pH meter. The pH was recorded to be at pH 5.03.



Figure 3.9: Prepared 200mL Zinc-Nickel Alloy Bath Solution

20. The prepared solution as shown in Figure 3.9 was then poured into 250mL Scott Bottle for storage as illustrated in Figure 3.10 to be used later during electrodeposition.



Figure 3.10: Zinc-Nickel Alloy Solution in 250mL Scott Bottle

### 3.2.4 Zinc-Nickel Alloy Electrodeposition Process

Substrate or the working electrode in this experiment is API 5L X52 carbon steel. The low carbon steel plate was cut into 5 pieces of required surface area dimension ( $1\text{ cm}^2$ ) and mounted with epoxy resin. A copper wire is then physically made in contact to the electrode through soldering. This procedure for sample preparation is shown in Figure 3.11.

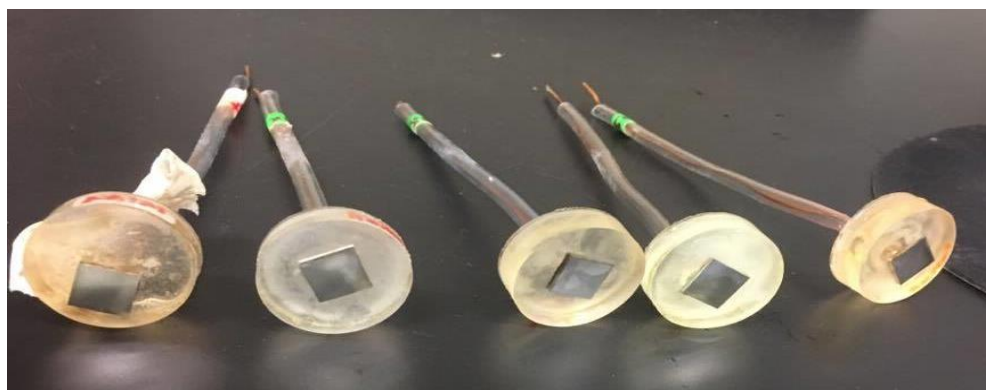


Figure 3.11: Mounted X52 low carbon steel

The low carbon steel electrodes mounted with epoxy resin then underwent grinding and polishing process before the start of electrodeposition to remove rust, unwanted material at the area of interest and damage from cutting. A grinder-polisher machine as shown in Figure 3.12 was used for this process.



Figure 3.12: Grinder-Polisher Machine

Initial grinding is done with the coarse 120 grit SiC paper followed by 240, 320, 400, 600, 800 and to a very fine 1200 grit SiC paper. This grinding process is illustrated in Figures 3.13 to Figure 3.15.



Figure 3.13: Process of grinding



Figure 3.14: Sample Surface before grinding

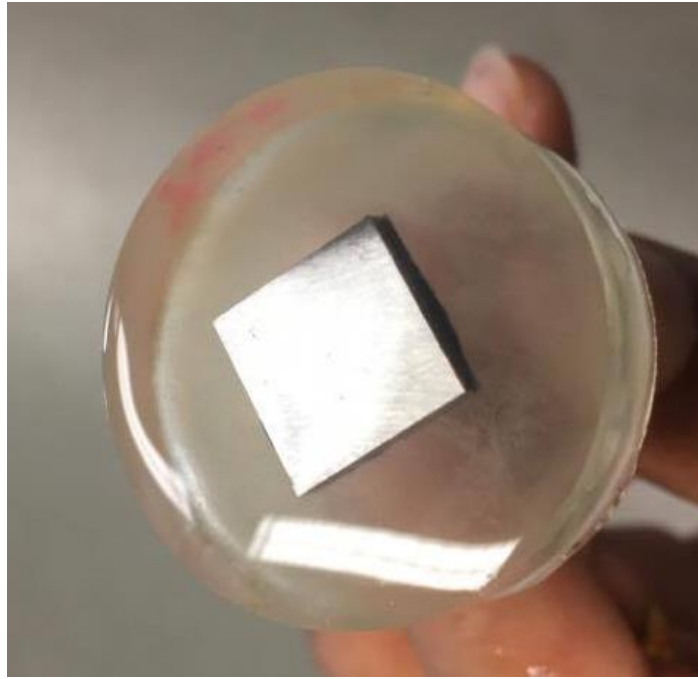


Figure 3.15: Sample surface after grinding up to 1200 grit SiC paper

The grinded samples were then polished with polycrystalline diamond suspensions. Polycrystalline diamond provides better surface finish and higher material removal rates for metallographic sample preparation. Polishing was done on the carbon steel samples to allow better adhesion of coating on the metal surface during the process of electrodeposition. Initial rough polishing was done using 3  $\mu\text{m}$  polycrystalline followed by a final polishing using 1  $\mu\text{m}$  polycrystalline diamond. Few drops of polycrystalline diamond were administered on the polishing cloth and the sample was placed on the region of diamond drops and polished in a figure of eight manner. The samples were polished until a mirror-like surface finish is obtained. The polished samples were then cleaned with acetone, clean water and dried at room temperature as a part of metal surface preparation. The polishing process is shown in FigureF 3.16 to Figure 3.21.

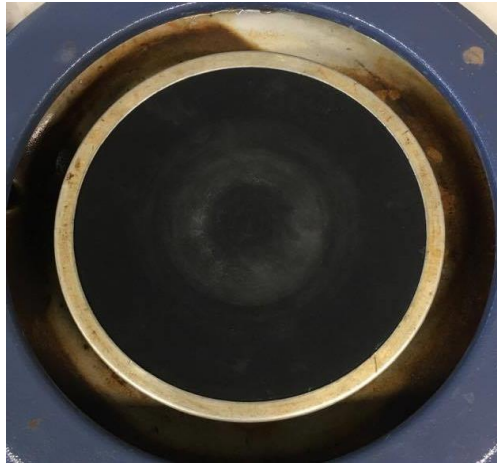


Figure 3.16: Polishing paper



Figure 3.17: Rough polishing (3  $\mu\text{m}$  polycrystalline diamond suspension)



Figure 3.18: Final polishing (1  $\mu\text{m}$  polycrystalline diamond suspension)



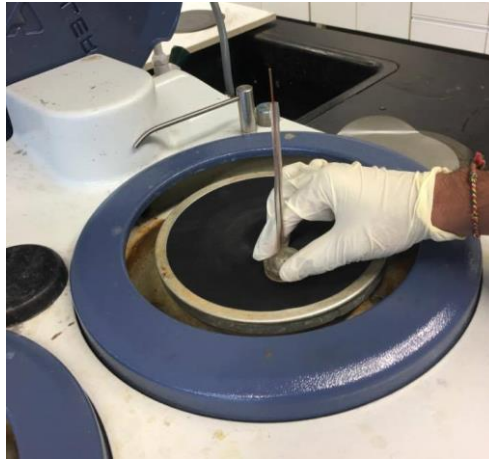


Figure 3.19: Polishing process in figure of eight manner

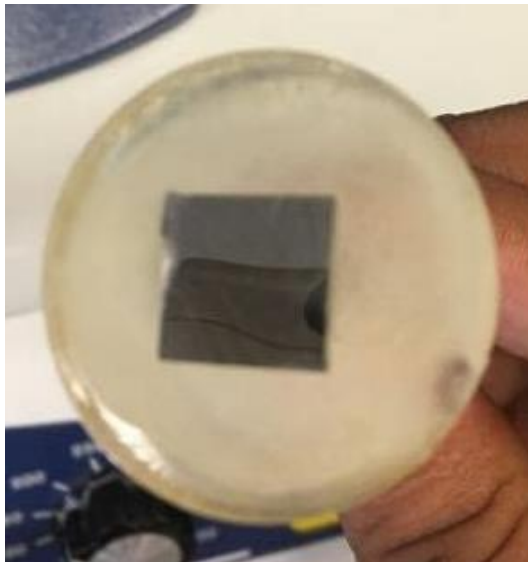


Figure 3.20: Mirror-like surface finish of sample after polishing process

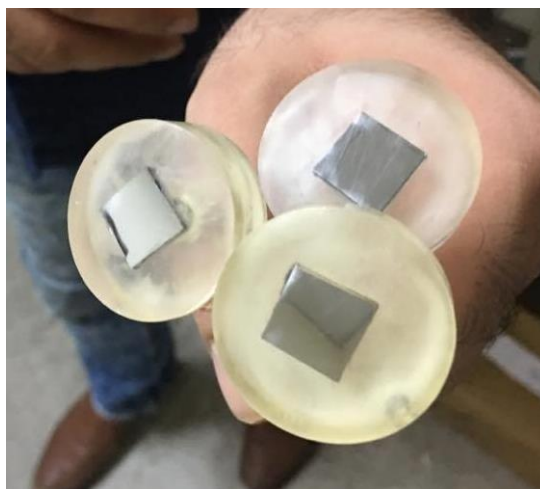


Figure 3.21: Samples after polishing

Electrochemical deposition is employed in this project. The working electrode is API 5L X52 low carbon steel, the reference electrode being Ag/AgCl and a mesh Pt is used as the counter electrode. Electrodeposition process of four cycles, one for each deposition temperature are carried out galvanostatically [31]. The technique used for electrodeposition is chronopotentiometry.

Following are the experimental procedure for the zinc-nickel electrodeposition:

- 1) The zinc-nickel chloride bath solution stored in scott bottle is poured into a 250mL beaker.
- 2) The bath solution is stirred using magnetic stirrer at 300 to 500 revolutions per minute (rpm) to allow mixture of solution to dissolve.
- 3) The experimental setup for electrodeposition is done. Figure 3.22, 3.23, 3.24 and 3.25 illustrates the experimental setup for electrodeposition at different temperatures.
- 4) The chronopotentiometry procedure for electrodeposition is set up in the NOVA software with the electrodeposition parameters presented in Table 3.1.
- 5) The electrodes were connected to Metrohm Autolab galvanostat and the experiment is started.
- 6) This procedure is repeated for all four samples deposited at 25°C, 40°C, 60°C and 70°C. For temperature above 25°C, the temperature is consistently monitored during the process of electrodeposition.

Table 3.1: Electrodeposition parameters

Bath composition	Quantity	Electrodeposition parameters
ZnCl <sub>2</sub>	80 g/l	Temperature (T): 25°C, 40°C, 60°C and 70°C
NiCl <sub>2</sub> ·6H <sub>2</sub> O	110 g/l	Current density (j): 10 mA/cm <sup>2</sup>
NH <sub>4</sub> Cl	220 g/l	Agitation speed (R): 300 rpm
		Deposition time: 60 minutes
		pH = 5.0 (adjusted by adding ammonia)



The instrument used for electrochemical deposition is the Metrohm Autolab potentiostat/galvanostat and a hot plate with stirrer to adjust the bath agitation or stirring rate and temperature as per required for each electrodeposition.

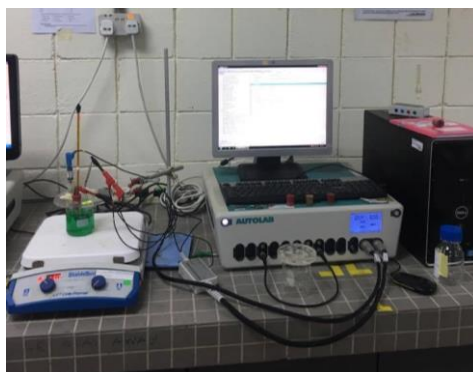


Figure 3.22: Metrohm Autolab Potentiostat/Galvanostat with experimental setup for zinc-nickel alloy electrodeposition

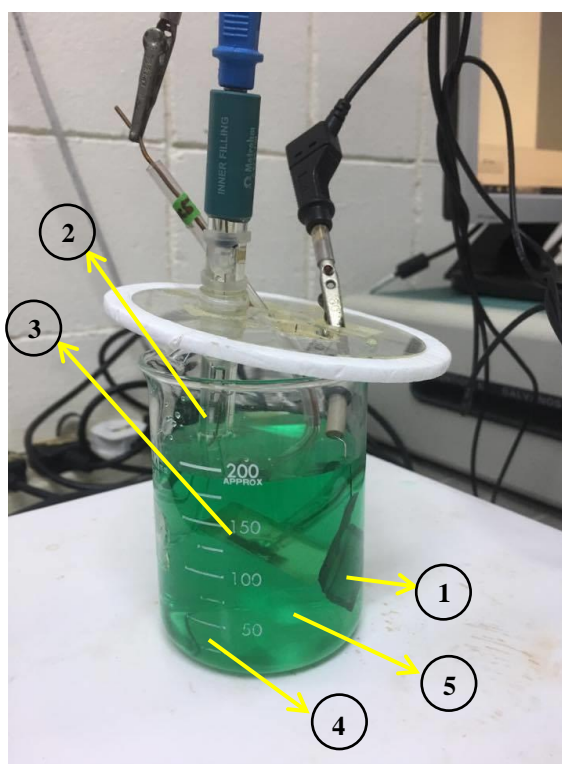


Figure 3.23: Electrodeposition Setup for 25°C

- (1) Pt mesh counter electrode, (2) Ag/AgCl reference electrode,
- (3) Epoxy mounted low carbon steel (working electrode),
- (4) Zinc-Nickel Alloy Bath Solution, (5) Magnetic Stirrer



Figure 3.24: Setup for Electrodeposition at temperature 40°C, 60°C and 70°C

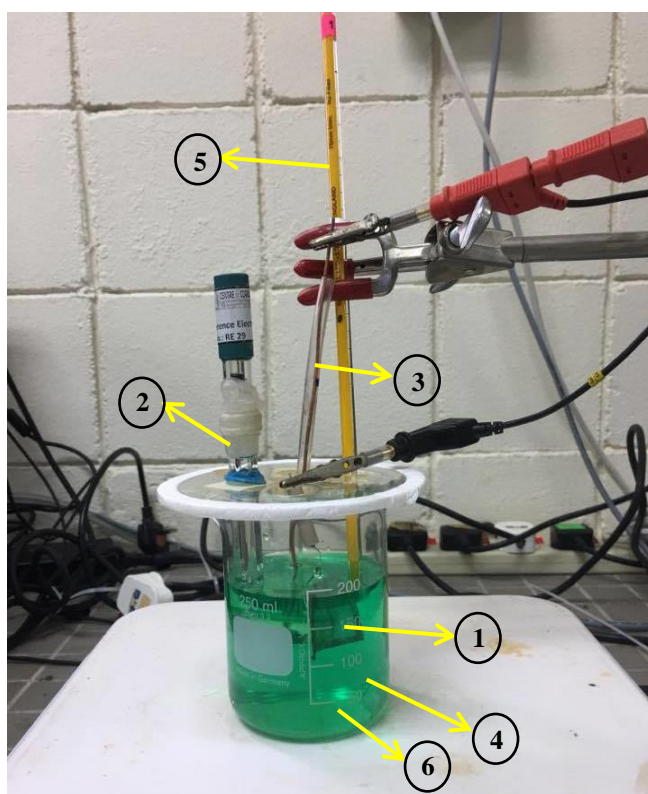


Figure 3.25: Electrodeposition Setup for 40°C, 60°C and 70°C

- (1) Pt mesh counter electrode, (2) Ag/AgCl reference electrode
- (3) Epoxy mounted low carbon steel (working electrode),
- (4) Zinc-Nickel Alloy Bath Solution,
- (5) Thermometer, (6) Magnetic stirrer

### 3.2.5 SEM Analysis

The electrodeposited zinc-nickel alloy coatings on carbon steel substrate is analysed on its microstructural and compositional properties using the SEM.

The SEM and the computer are switched ON. The electrodeposited zinc-nickel alloy sample is put in a holder and put inside the SEM. The image of common morphology observed in the electrodeposited zinc-nickel alloy sample is captured and the observed microstructure and various spots identified are analysed using EDX to observe the elemental composition of the spots identified. The image and data observed by the SEM and EDX is saved in the computer. The procedure is repeated for all samples coated with zinc-nickel alloy at 25°C, 40°C, 60°C and 70°C.

### 3.2.6 LPR Analysis

For electrochemical corrosion tests, the zinc-nickel alloy coating samples electrodeposited at different temperatures are immersed into 3.5% NaCl solution simulating the seawater or marine environment.

Following are the experimental procedure for LPR measurement:

1. 35 g of NaCl was added to 1000mL of deionized water. The mixture of solution was stirred until dissolved. The mixture of solution is then poured into glass cell. This is illustrated in Figure 3.26.



Figure 3.26: Preparation of 3.5 wt% NaCl solution

2. The three-electrode electrochemical experimental setup is done. Figure 3.27 illustrates the experimental setup and placement of the electrodes.

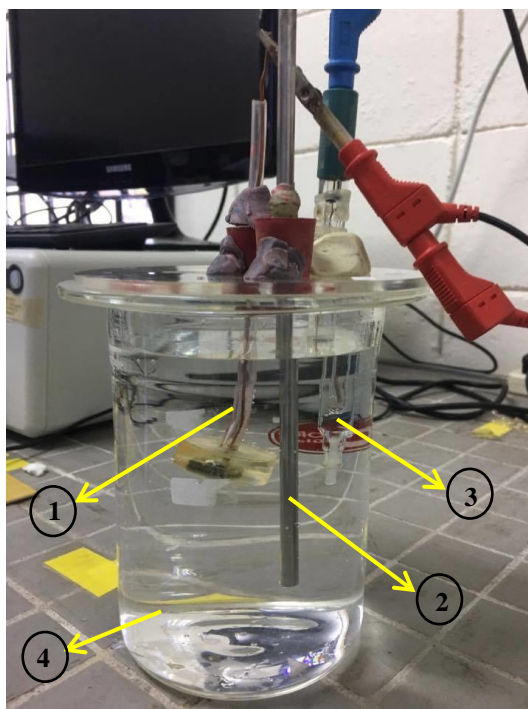


Figure 3.27: Three-electrode electrochemical setup for LPR Analysis

(1) Zn-Ni coated sample, (2) Stainless steel counter electrode

(3) Ag/AgCl reference electrode, (4) 3.5 wt% NaCl solution

3. The LPR procedures are set up, the electrodes are then connected to the Metrohm Autolab potentiostat as shown in Figure 3.28 and the experiment is started.

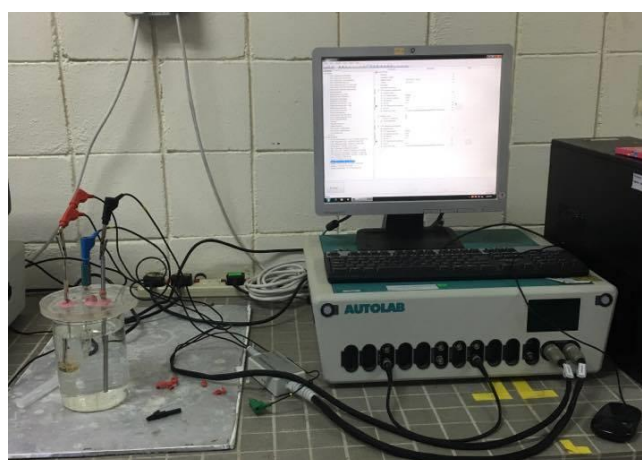


Figure 3.28: Metrohm Autolab Potentiostat/Galvanostat with experimental setup for LPR Analysis

4. Five samples are subjected to corrosion rate measurement. One sample out of the five samples would not be coated and used as a plain carbon steel reference sample to be used to study and compare the results of corrosion rate of 4 coated samples at different temperature vs. the plain carbon steel reference sample.
5. The open circuit potential (OCP) is stabilized for 30 minutes. This stabilization process is done before each reading is taken.
6. For LPR experiments, readings are taken every hour for 24 hours. The corrosion potential is first measured, and subsequently sweeping from -10 mV to +10 mV with sweep rate of 10 mV/min.
7. This procedure is repeated for a plain carbon steel reference sample and all four samples deposited at 25°C, 40°C, 60°C and 70°C.

### **3.2.7 Corrosion rate (CR) and Composition Reference Line (CRL) calculation**

Composition reference line separates anomalous and normal co-deposition type. Composition Reference Line is calculated based on the following equation:

$$CRL = \frac{c(Ni^{2+})}{c(Ni^{2+} + Zn^{2+})} \quad (3.1)$$

where  $c(Ni^{2+})$  and  $c(Zn^{2+})$  are the nickel and zinc ion composition in the bath.

The polarization resistance ( $R_p$ ) data obtained from LPR would be used to evaluate the corrosion rate of the steel. The corrosion rate in mm/yr is calculated based on the following equations with reference to the standard provided (ASTM G59):

$$R_p = \frac{\Delta E}{\Delta I} \quad (\text{slope of potential to current plot}) \quad (3.2)$$

From Metroehm Autolab potentiostat data, polarization resistance ( $R_p$ )

$$R_p = \frac{1}{\text{slope}} (\Omega) \quad (3.3)$$

Corrosion current,  $i_{\text{corr}}$ ,

$$i_{\text{corr}} = \frac{B}{R_p} \quad (3.4)$$

where B is Stern-Geary constant which is given a value of 26 millivolt (mV).

Corrosion rate (mm/yr) is calculated based on the equation:

$$\text{Corrosion Rate} = K \cdot EW \cdot \frac{i_{\text{corr}}}{\rho \cdot A} (\text{mm/yr}) \quad (3.5)$$

Where

K = constant that defines the unit for corrosion rate

EW = Equivalent weight of the steel (X52 carbon steel)

$\rho$  = Density of the steel

A = Exposed Surface area of the steel

### 3.3 Key Milestones

Following are the key milestones listed according to semester weeks for Final Year Project 1 and 2:

Table 3.2: Key Milestone for FYP 1

No	Key Milestone	Weeks	FYP
1	Selection of topic	1	1
2	Submission of Extended Proposal	4	
3	Proposal Defence	6	
4	Acquire Materials Required and Experiment Preparation	13	
5	Submission of Interim Draft Report	13	
6	Interim Report Submission	14	

Table 3.3: Key Milestone for FYP 2

No	Key Milestone	Weeks	FYP
1	Submission of Progress Report	7	2
2	Pre-SEDEX	10	
3	Submission of Draft Final Report	11	
4	Submission of Dissertation (Soft bound)	12	
5	Submission of Technical Paper	12	
6	Oral Presentation	13	
7	Submission of Project Dissertation (Hardbound)	15	

### 3.4 Gantt Chart

This chapter outlines the Gantt chart for Timeline for Final Year Project 1 and 2.

Table 3.4: Gantt Chart for Timeline for FYP 1

Project Work	Weeks													
	Final Year Project 1													
	1	2	3	4	5	6	7	8	9	10	11	12	13	14
Selection of topic														
Early Research Work on Literature														
Submission of Extended Proposal														
Proposal Defence														
Acquire Materials Required and Experiment Preparation														
Submission of Interim Draft Report														
Interim Report Submission														


Progress


Key Milestone



Table 3.5: Gantt Chart for Timeline for FYP 2

Project Work	Weeks														
	Final Year Project 2														
	1	2	3	4	5	6	7	8	9	10	11	12	13	14	15
Sample Preparation															
Experiment Conduct															
Submission of Progress Report															
Pre-SEDEX															
Experimental Result Analysis															
Full Result Documentation															
Submission of Draft Final Report															
Submission of Dissertation (Soft Bound)															
Submission of Technical Paper															
VIVA															
Submission of Dissertation (Hard Bound)															

 Progress

 Key Milestone

## **CHAPTER 4: RESULTS AND DISCUSSION**

The results of the experiments conducted are presented and discussed in this chapter.

### **4.1 Results and Discussion**

Temperature variation during electrodeposition impacts the deposition rate as metal ion diffusion from bath electrolyte to the working electrode or cathode is increased with temperature whereby temperature increase by 1°C results in a 10% increase in electrochemical or deposition rate and 2% rate of mass transfer improvement in most cases and very high temperature leads to hydrogen evolution and low temperature leads to porosity or lesser uniformity and compactness due to low deposition rates [8]. This in turn impacts the corrosion resistance of zinc-nickel alloy coatings. These changes are observed during microstructural, compositional analysis and corrosion resistance measurement. The presence of micro-cracks, compactness, uniformity, surface morphologies and the percentage compositions of each metals (zinc and nickel) in the deposited alloy is analysed through SEM and EDX and corrosion measurement through LPR. This section presents the results and discussion on the influence of deposition temperature on the corrosion resistance of electrodeposited zinc-nickel alloy.

#### **4.1.1 Electrodeposition process**

The zinc-nickel alloy coatings had been electrodeposited onto the carbon steel substrate at 25°C, 40°C, 60°C and 70°C using the technique of chronopotentiometry with the parameters as mentioned in the chapter 3.24. The potential-time graph at different temperatures for the electrodeposition process are shown in Figure 4.1.

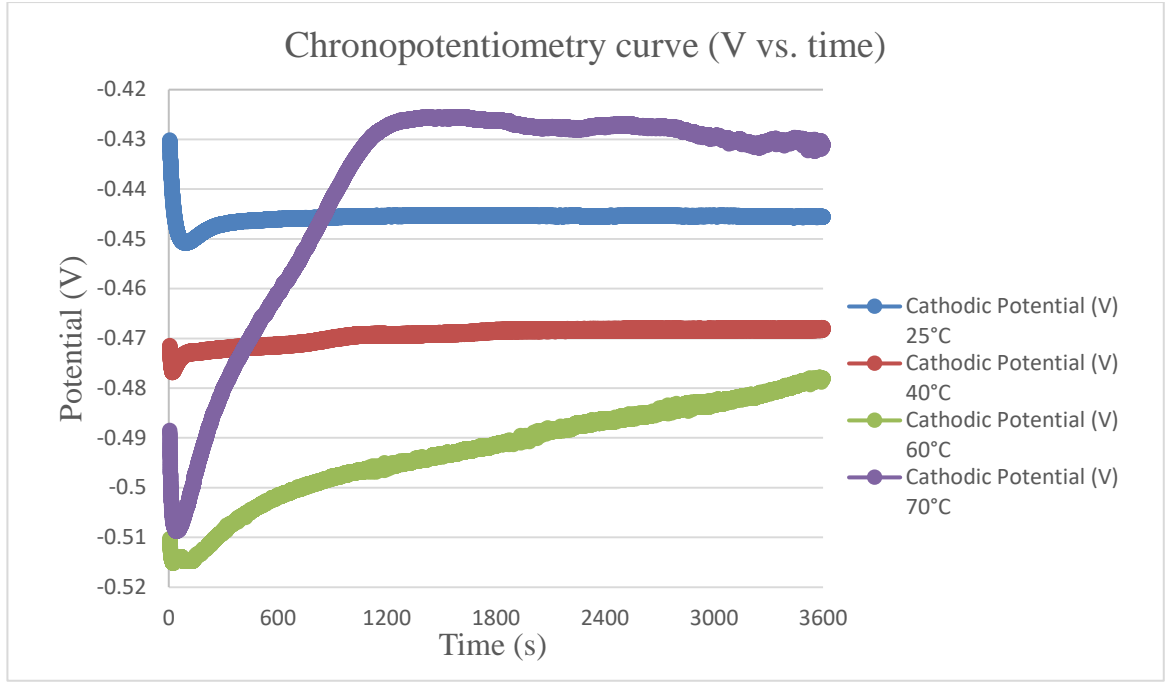


Figure 4.1: Zinc-nickel deposition potential vs. time graph obtained at different temperatures of 25°C, 40°C, 60°C and 70°C

The potential vs time graph for deposition of zinc-nickel at 25°C, 40°C, 60°C and 70°C were observed throughout the electrodeposition process. Although initially a drop in cathodic potential was observed as the temperature is increased, with time, the graphs showed increase in cathodic potential with increase in time up to 60 minutes. A straight horizontal line graph with slight to no increase in cathodic potential is observed with time for deposition at 25°C. With increase in temperature to 40°C, a linearly increasing line of potential vs. time at 40°C in Figure 4.1 was observed which indicates increase in cathodic potential with time. As with deposition at 60°C, larger increase in cathodic potential is observed with time which is observed by larger slope increase in the line of potential vs. time in Figure 4.1 at 60°C. When the deposition temperature is increased to 70°C, drastic increase in potential vs. time graph was observed as in Figure 4.1 which reaches its maximum at -0.425V at the 1400th second and then a slight drop in cathodic potential is observed.

The increase in cathodic potential with time is observed with increase in temperature. Cathodic potential in chronopotentiometry for electrodeposition is attributed to the concentration of ions getting reduced at the metal substrate surface in response to the applied current. As mentioned in [32], the measured potential changes as a

concentration overpotential is developed with time when the concentration of reactants decreases getting reduced to the substrate surface. The measured potential changes with time increasing or decreasing depending on the ratio of concentration between reactants and products on the metal substrate surface. As the concentration of electrolyte ions decrease at the metal substrate surface as a result of the reduction process, a concentration gradient is developed between the ions in the bath solution and the metal substrate surface which results in the ions to diffuse down the concentration gradient from a higher concentration in bath to a lower concentration on metal surface and this change in concentration with time results in change in potential vs. time graph. As time passes, the concentration of ions on metal surface becomes zero at which this reduction reaction can no longer support the applied current which will result in large potential change due to the reduction reaction of another ion on the metal surface to support the applied current [33]. This relationship of deposition potential change with time as the concentration of reactant changes is expressed in the following equation (4.1):

$$E = E^{\circ} + \frac{0.059}{n} \log \frac{C^s_O}{C^s_R} \quad (4.1)$$

$C^s_O$  and  $C^s_R$  indicates the concentration of reactants and products on metal surface.

The standard reduction potential  $E^{\circ}$  (V) for nickel reduction is -0.25 vs. SHE and the standard reduction potential  $E^{\circ}$  (V) for zinc reduction is -0.76 vs. SHE. The cathodic potential observed in the chronopotentiometry curve is close to the standard reduction potential  $E^{\circ}$  (V) of the reactants that gets reduced to its metal on the surface by accepting electrons. Hence, observations on the increase in cathodic potential towards more positive value with time for electrodeposition at 60°C and 70°C indicates the deposition cathodic potential moving closer to  $E^{\circ}$  (V) of nickel reduction favouring the process of nickel reduction to its metal at the substrate surface. This assumption is further supported by EDX results.

The increase in nickel content is attributed to increase in cathodic potential with time during the process of electrodeposition. This assumption is supported by [34], who mentioned on the increase in cathodic potential with increasing nickel concentration

in the bath leading to increase in nickel deposition and [30] who observed similar results of increasing cathodic potential with increasing nickel content in the deposited coating with temperature. The potential vs. time graph obtained correlates with the EDX result on the elemental composition obtained for zinc-nickel alloy coating deposited at different temperature with increase in nickel content in the coatings with increase in temperature as a result of increase in cathodic potential. Further research done by [30] on applying fixed constant potential (potentiostatic method) in the process of electrodeposition at different temperatures observed only slight increase in nickel content (below 20%) even at high temperatures at 70°C as to compared with the chronopotentiometry method where increase in nickel content is observed with increase in cathodic potential with temperature. This further supports the assumption. As for the graph obtained at 70°C, a maximum value is reached before the maximum electrodeposition time of 3600 seconds is achieved which indicates saturation coverage or complete occupancy of the deposit on the metal surface. The number of reactants, nickel and zinc ions reducing to product has reached saturation point whereby the concentration of reactants has been reduced to zero at the metal surface halting the reduction reaction of the reactants.

#### **4.1.2 Electrodeposited zinc-nickel alloy coatings**

This chapter illustrated the visual observation of the coatings formed from electrodeposition at different temperatures of 25°C, 40°C, 60°C and 70°C. Images of coatings formed at 25°C, 40°C, 60°C and 70°C are presented in the figures 4.2 to 4.5.

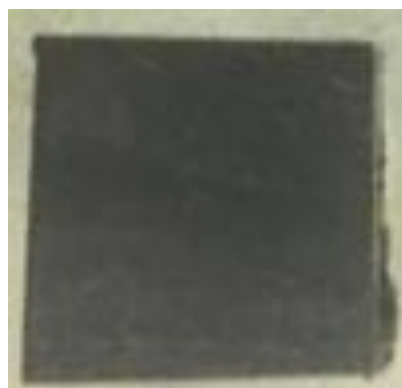


Figure 4.2: Zinc-nickel alloy coating formed for electrodeposition at 25°C

Visual observation done on the coating formed at 25°C, it was observed that the colour of the deposit is 'dark greyish'. This dark grey colour coating might be attributed to the colour that is formed when the blue-grey zinc deposits on the silvery carbon steel as EDX analysis in chapter 4.1.3 indicates prevalent zinc metal deposition compared to nickel at lower temperatures.

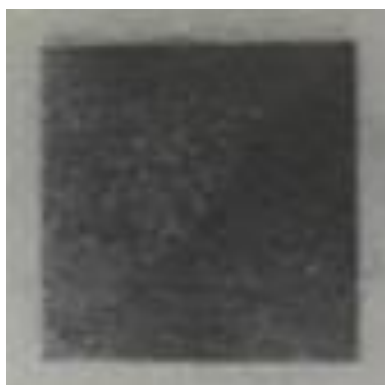


Figure 4.3: Zinc-nickel alloy coating formed for electrodeposition at 40°C

Visual observation on coatings deposited at 40°C showed similar observations on the colour of the deposit which is of 'dark greyish'.



Figure 4.4: Zinc-nickel alloy coating formed for electrodeposition at 60°C

Coatings deposited at 60°C was of lustrous 'silvery-white' in colour. This silvery-white is attributed to the colour of nickel metal and this is further confirmed by EDX analysis which indicates prevalent nickel formation when compared to zinc at higher temperatures.



Figure 4.5: Zinc-nickel alloy coating formed for electrodeposition at 70°C

Coatings deposited at 70°C showed similar observations on the colour and appearance of the deposit which of lustrous ‘silvery-white’.

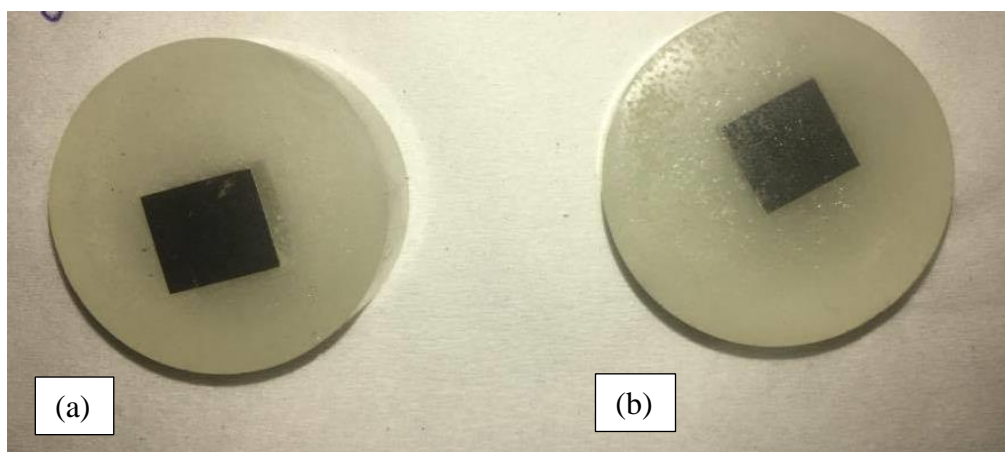


Figure 4.6: Images of coating formed at (a) 25°C and (b) 40°C

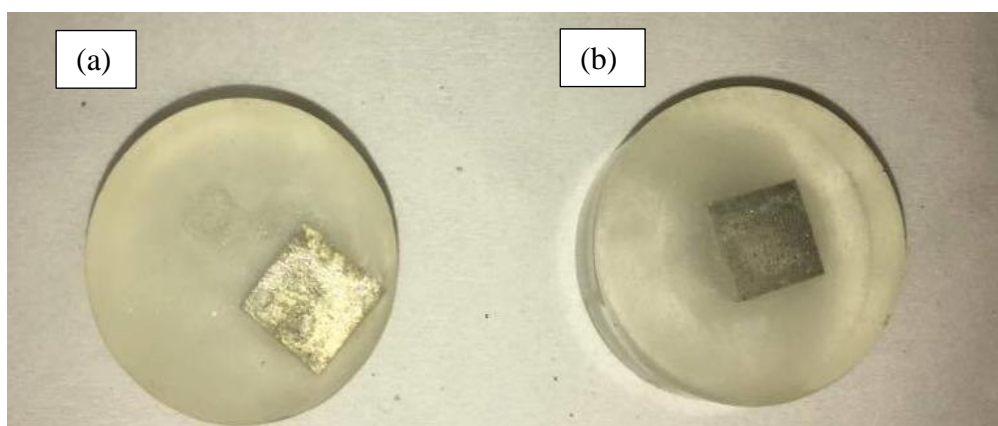


Figure 4.7: Images of coating formed at (a) 70°C and (b) 60°C

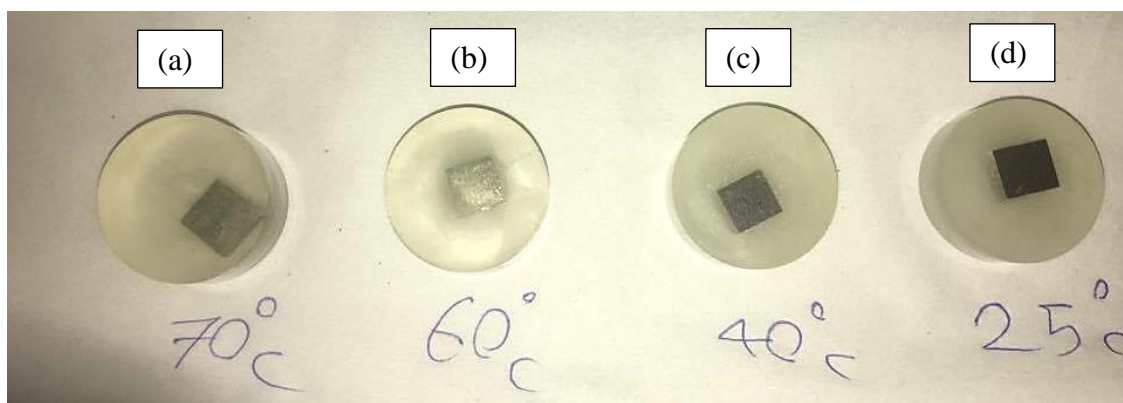


Figure 4.8: Images of coatings deposited at (a) 70°C, (b) 60°C, (c) 40°C and (d) 25°C

Indication of the type of deposit metals formed can be seen through visual observation on the colour of the deposit obtained at different temperatures. This is further confirmed by EDX analysis on the coated samples which provides accurate information on the type of metal deposited on the coated samples. This supports the visual observation of the coating deposit colour. Further analysis on the microstructure and elemental composition is done for better understanding of the coating which is discussed in chapter 4.1.3.



### 4.1.3 SEM and EDX Analysis

This chapter presents discussion on the surface morphology and elemental compositional analysis results obtained using SEM-EDX technique. Images from SEM-EDX are later analysed and correlated with measurement of corrosion rate to study on the corrosion resistance of zinc-nickel alloy coatings.

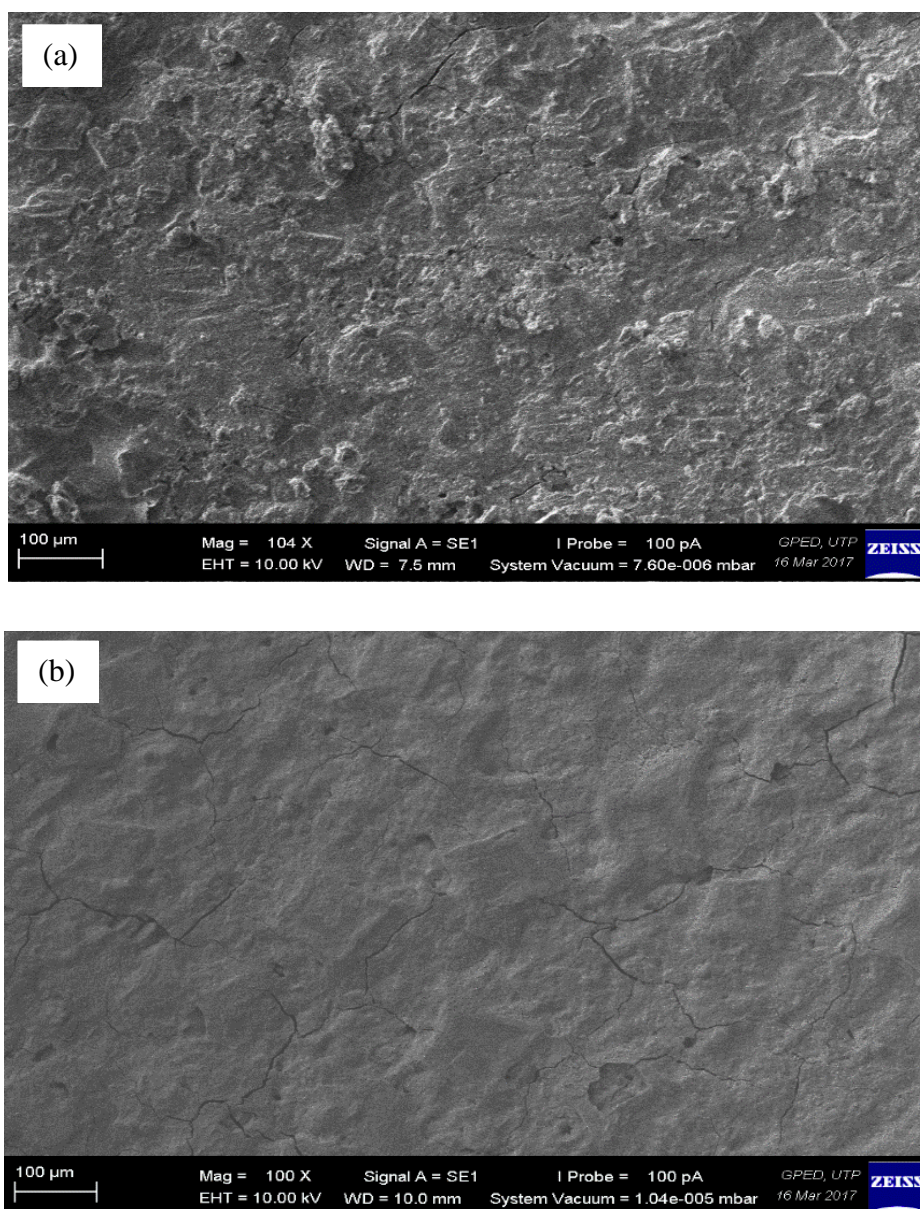


Figure 4.9: SEM images for electrodeposited zinc-nickel alloy coatings at (a) 25°C and (b) 40°C at magnification of 100x

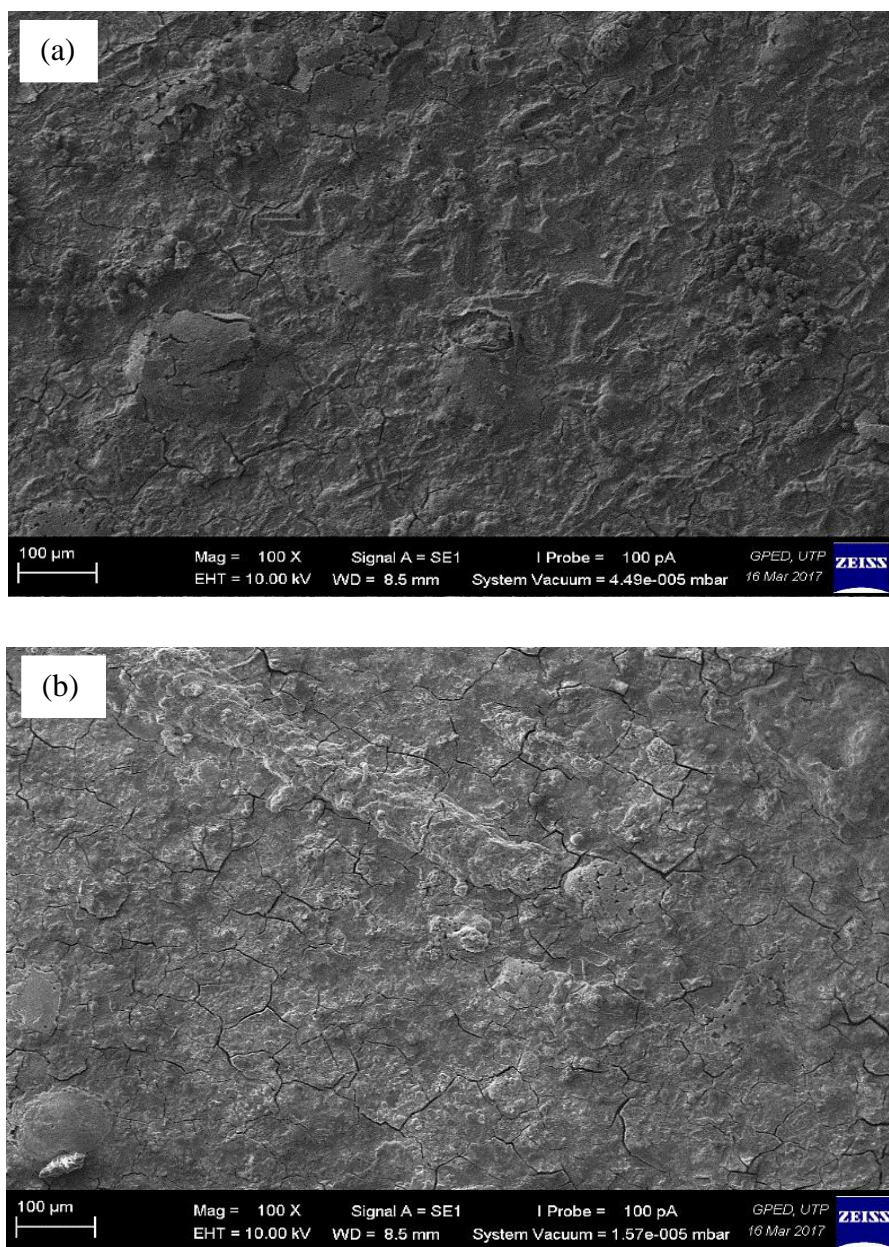


Figure 4.10: SEM images for electrodeposited zinc-nickel alloy coatings at (a) 60°C and (b) 70°C at magnification of 100x

It can be seen from the SEM images shown in Figure 4.9 and 4.10 that micro-cracks are observed in all the coatings deposited at different temperatures. The intensity of these microcracks are observed to increase with increasing deposition temperature, with coatings deposited at 70°C > 60°C > 40°C > 25°C. The formation of micro-cracks can be attributed to internal stress developed during the process of electrodeposition. Development of internal stress during electrodeposition can be related to many factors. The presence of micro-cracks in deposited zinc-nickel alloy coatings was observed when the nickel content in the coating increases in the alloy [35]. The presence of



micro-cracks in deposited zinc-nickel alloy in acidic bath is related to hydrogen embrittlement through the process of hydrogen evolution [24, 30]. Study conducted by an author also observed increase in hydrogen evolution reaction with observations of increase in partial current density of hydrogen with rising temperature [30]. This process of hydrogen reduction causes diffusion of hydrogen atoms in coatings straining the crystal lattice resulting in high internal stress causing cracks. Hydrogen production through water electrolysis (hydrogen evolution) is also highly facilitated in acidic environment with the use of acidic bath during electrodeposition.

SEM microstructural images of coatings deposited at 25°C, 40°C, 60°C and 70°C at higher magnification are shown in Figure 4.11 to Figure 4.23 where the surface morphology and microstructure of the coatings is analyzed. Microstructural study refers to identification and analysis of nucleation and growth of crystals. The surface of the coatings is analyzed to identify the similar microstructures primarily observed at different parts of the coatings and EDX analysis were done to identify the elements involved related to the microstructure observed.

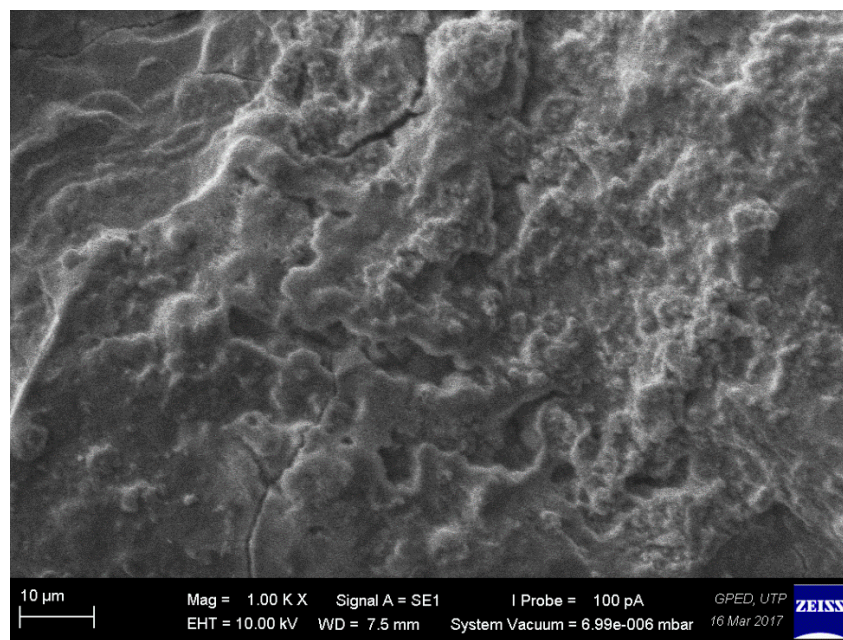


Figure 4.11: SEM image at 1000x magnification for zinc-nickel alloy coatings deposited at 25°C

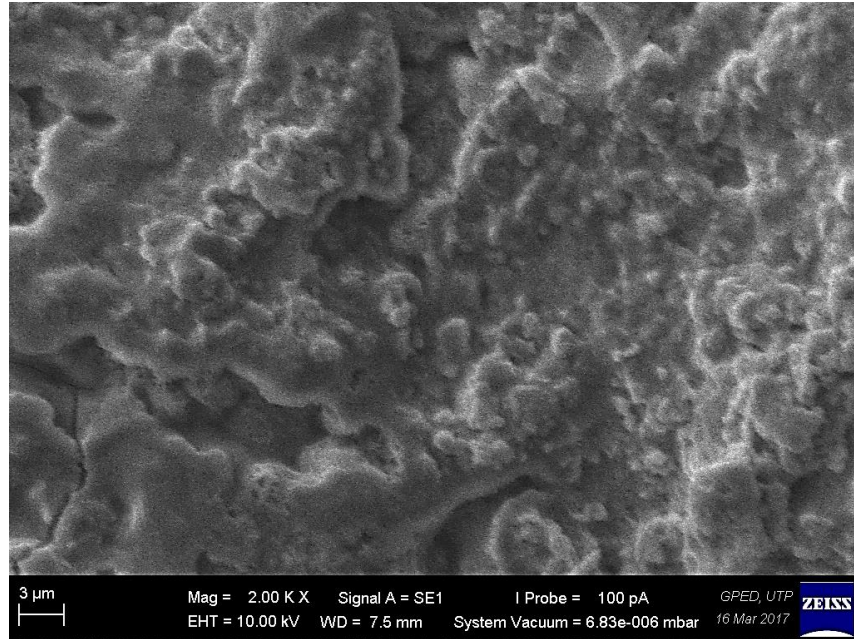


Figure 4.12: SEM image at 2000x magnification for zinc-nickel alloy coatings deposited at 25°C

Observations on the SEM images in Figure 4.11 and 4.12 at higher magnification revealed smaller grain size ( $0.5\mu\text{m}$  -  $1\mu\text{m}$ ) with dense and compact morphology. The grain structures observed are of fine irregular shape. EDX analysis shown in Figure 4.13 on the fine irregular shaped grain structure obtained from SEM reveals the composition of the element of zinc predominantly (88%) identified as seen in the first (a) part of the spectrum in Figure 4.13 and hence through EDX analysis the compact fine irregular shaped grain structure observed can be related to the microstructure of zinc.

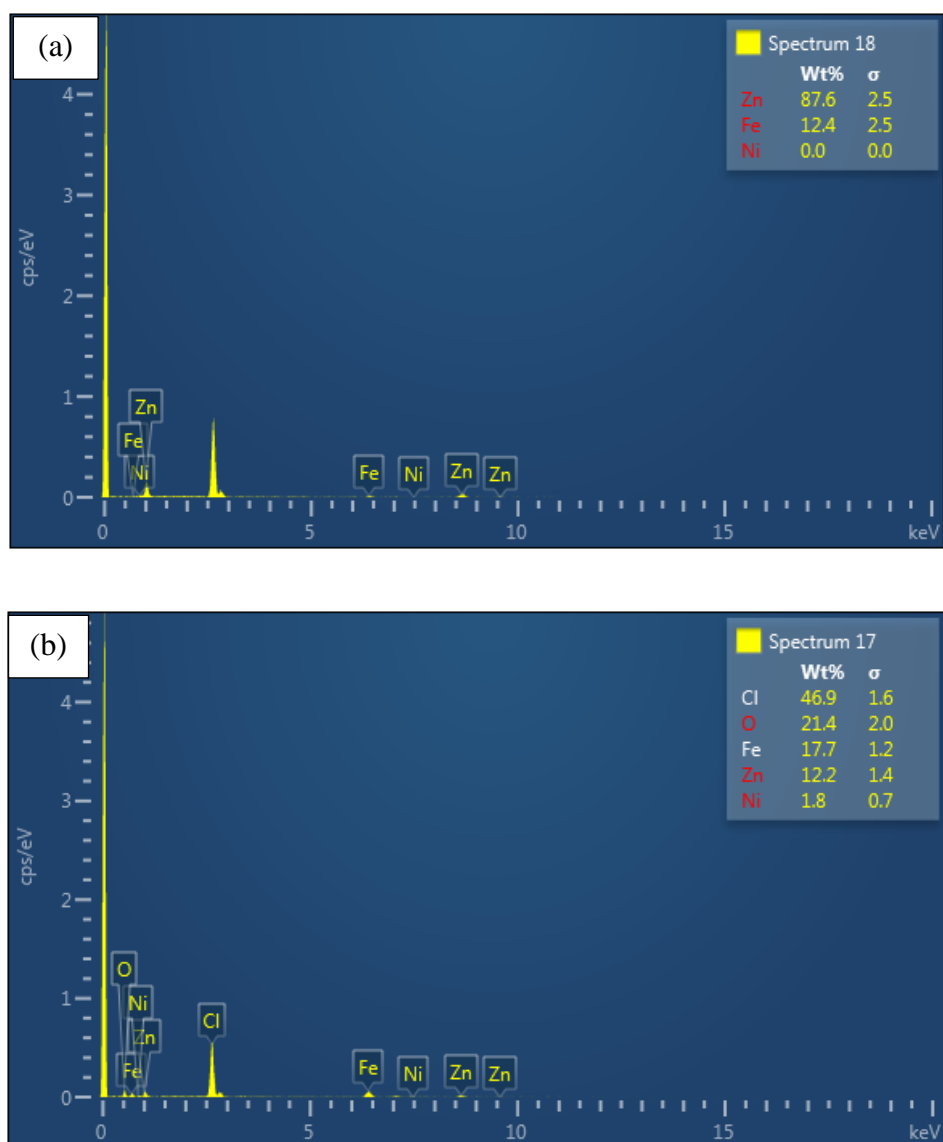


Figure 4.13: EDX Spectrum (a) and (b) for zinc-nickel alloy coatings deposited at 25°C

From the EDX spectrum data extracted from several points on the morphologies of the coatings, the average zinc-to nickel ratio weight percentage in the coatings at 25°C is observed to be 85 to 90% zinc and 10 to 15% nickel. There are also other elements' presence observed in the EDX spectrum which are oxygen, chlorine and iron besides zinc and nickel.

Shown in figure 4.14 and 4.15 are SEM images for coatings deposited at 40°C.



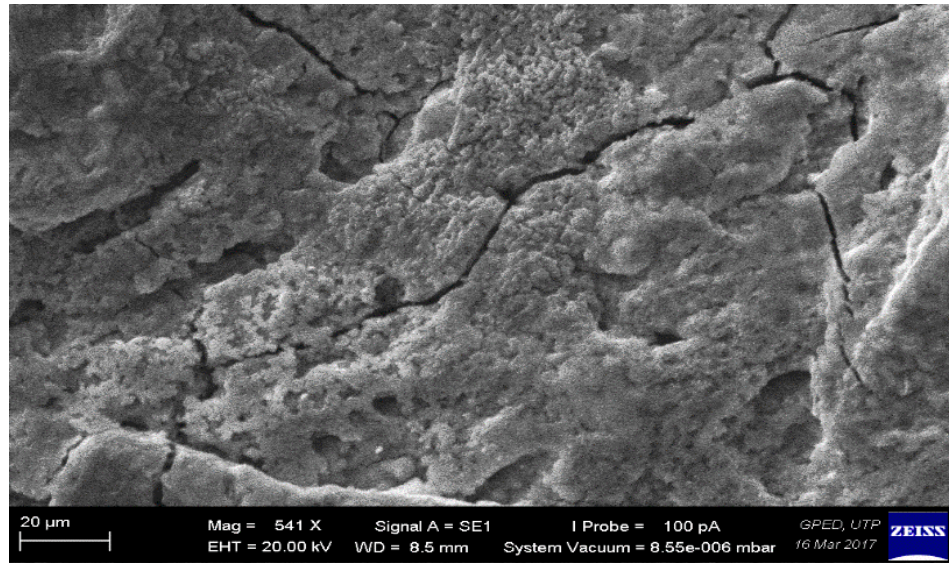


Figure 4.14: SEM image at 500x magnification for zinc-nickel alloy coatings deposited at 40°C

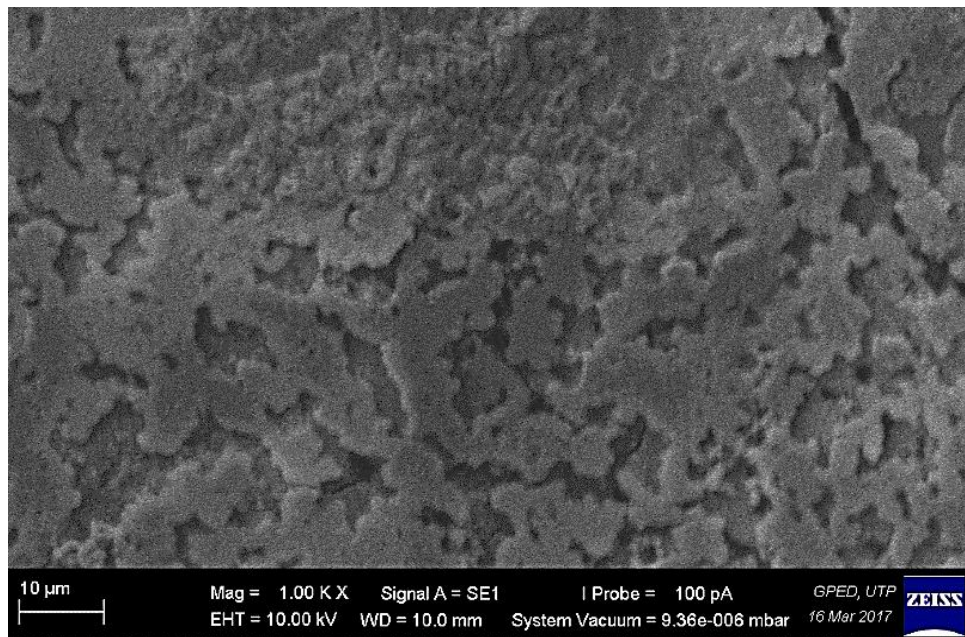


Figure 4.15: SEM image at 1000x magnification for zinc-nickel alloy coatings deposited at 40°C

Observations from the SEM image shown in Figure 4.14 reveals the presence of micro-cracks in the coating which is more clearly depicted as observed at 500x magnification and observations of the grain structures at 1000x magnification in Figure 4.15 are loosely arranged cauliflower structure and of larger grain size (2 μm to 5 μm). EDX analysis shown in Figure 4.16 on the loosely arranged cauliflower structure obtained

from SEM reveals a high percentage of iron element, followed by zinc and nickel. The presence of iron element (substrate) explains the loose arrangement of the grain structure which exposes the substrate to the surface and the cauliflower structure may be attributed to both zinc and nickel as the nickel content in the coating increases.

Figure 4.16 illustrates the spectrum obtained from EDX analysis.

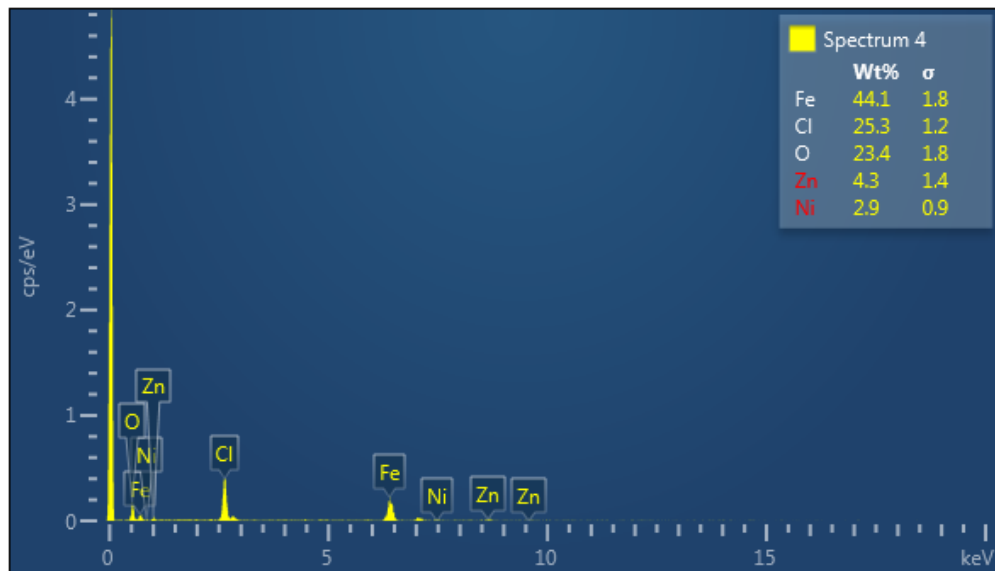


Figure 4.16: EDX Spectrum for zinc-nickel alloy coatings deposited at 40°C

From the EDX spectrum data extracted from several points on the morphologies of the coatings, the average zinc-to nickel ratio weight percentage in the coatings at 40°C is observed to be 60 to 70% zinc and 30 to 40% nickel. There are also other elements' presence observed in the EDX spectrum which are oxygen, chlorine and iron beside zinc and nickel.

Figures 4.17 and 4.18 shows the SEM images at higher magnification for coatings deposited at 60°C.



Figure 4.17: SEM image at 1000x magnification for zinc-nickel alloy coatings deposited at 60°C



Figure 4.18: SEM image at 3000x magnification for zinc-nickel alloy coatings deposited at 60°C

A more clearly depiction of deep micro-cracks is observed in Figure 4.17. Primary observation of lump forms of crystals nucleated and grown are seen during the process of microstructural analysing of the coating surface using SEM at various parts of the



coating surface. The grain structures observed at the crystals formed are of quadrangular shaped structure. Higher magnification (3000x) in Figure 4.18 reveals a quadrangular fibrous microstructure. EDX analysis shown in Figure 4.19 on the quadrangular fibrous microstructure revealed an elemental composition of nickel predominantly (85%) with small amount of zinc element present as observed in first (a) part of the spectrum in Figure 4.19 and hence through EDX analysis the quadrangular fibrous grain structure observed can be related to the microstructure of nickel.

The EDX spectrum were obtained from targeted several points on the morphology obtained from the SEM and the spectrum were analysed on the elemental composition present in the coatings. Figure 4.19 depicts the spectrum obtained from EDX analysis.

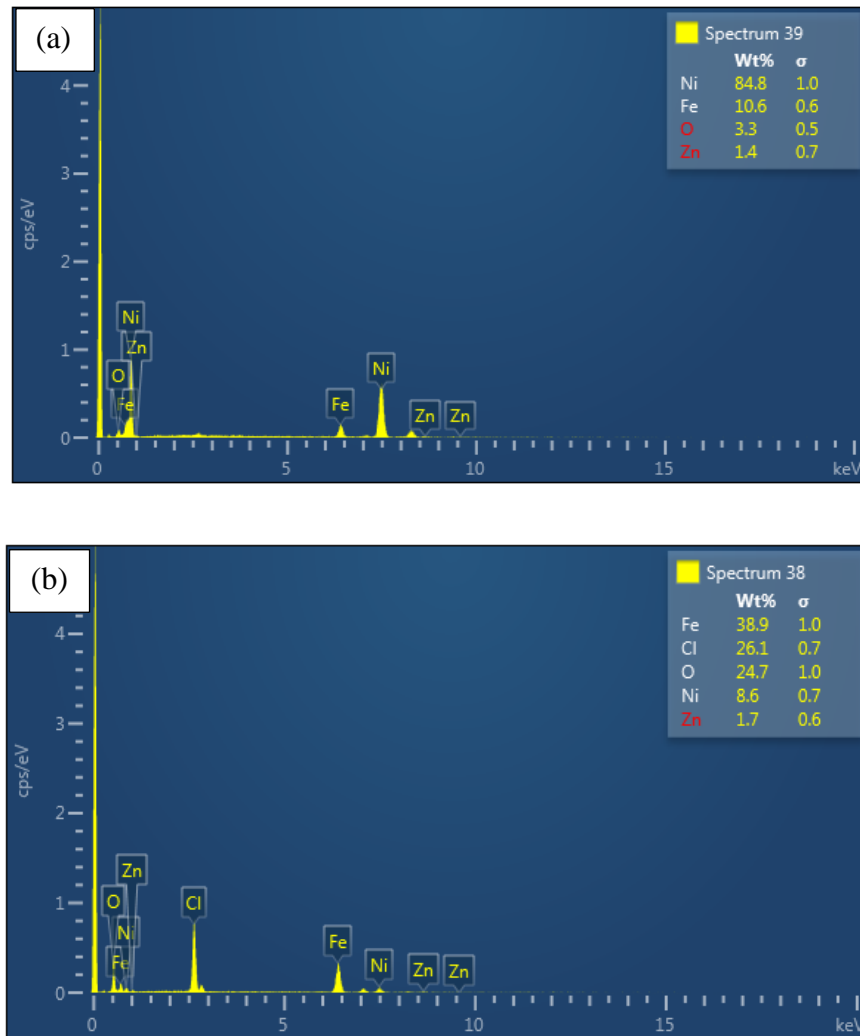


Figure 4.19: EDX Spectrum (a) and (b) for zinc-nickel alloy coatings deposited at 60°C

From the EDX spectrum data extracted from several points on the morphologies of the coatings, the average zinc-to nickel ratio weight percentage in the coatings at 60°C is observed to be 80 to 85% nickel and 15 to 20% zinc. Presence of oxygen, chlorine and iron were also observed in the EDX spectrum.

Figure 4.20, 4.21 and 4.22 illustrates the SEM images at higher magnifications for coatings deposited at 70°C.

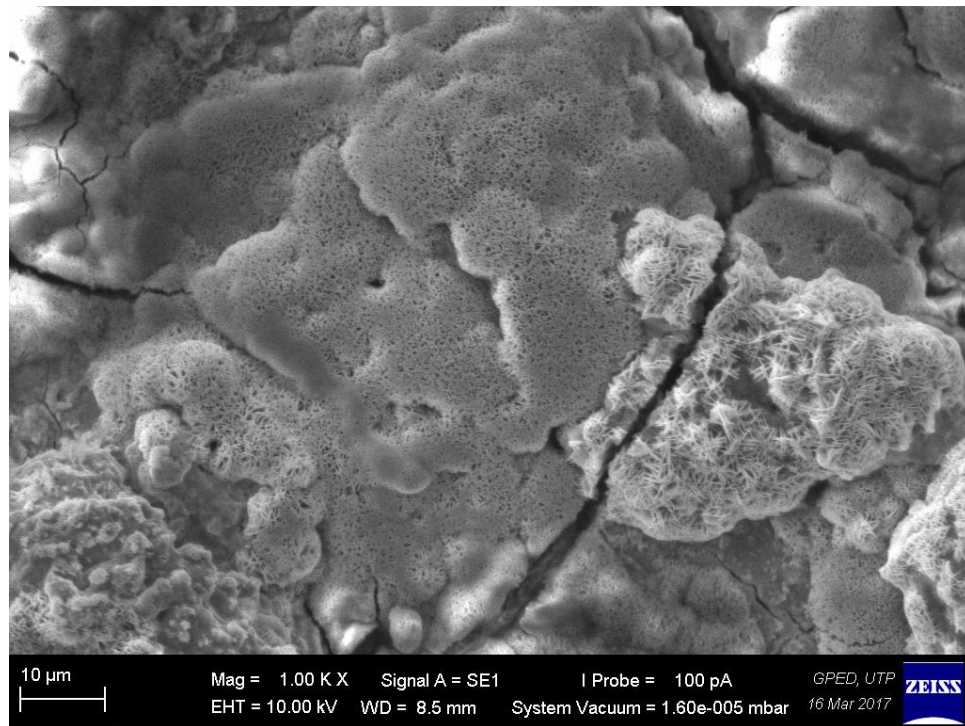


Figure 4.20: SEM image at 1000x magnification for zinc-nickel alloy coatings deposited at 70°C

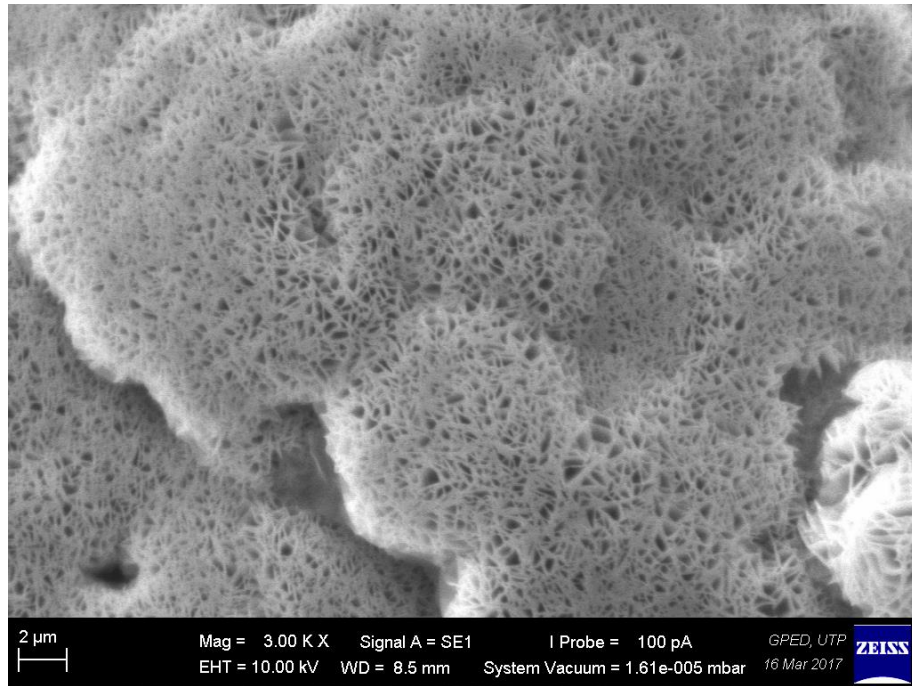


Figure 4.21: SEM image at 3000x magnification for zinc-nickel alloy coatings deposited at 70°C

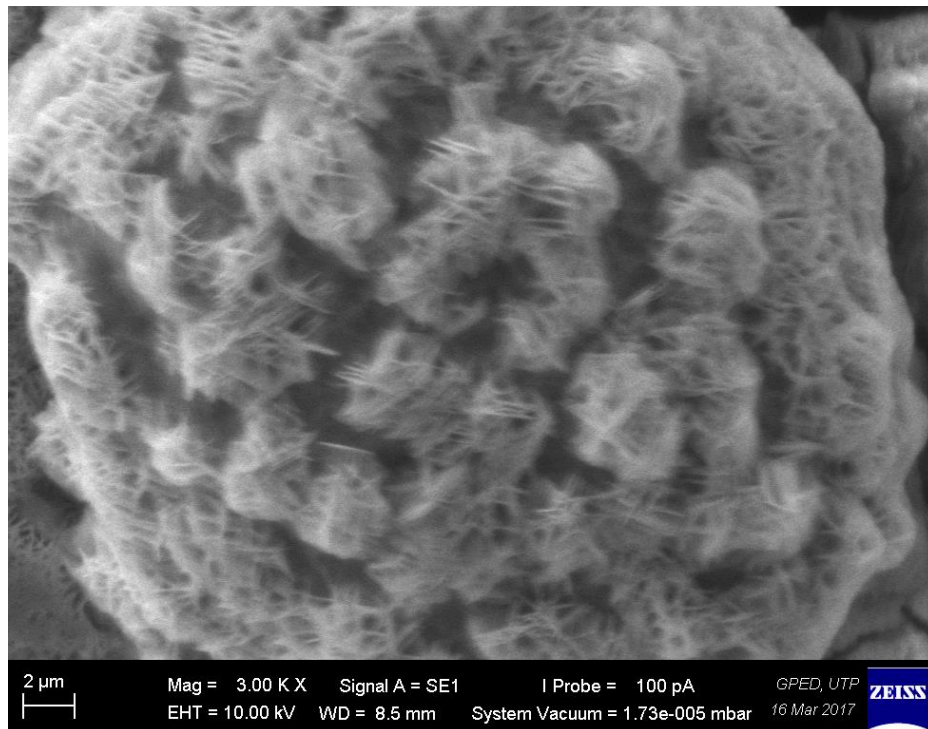


Figure 4.22: SEM image at 3000x magnification for zinc-nickel alloy coatings deposited at 70°C

Micro-cracks cutting through grain structures are observed in Figure 4.20. The micro-cracks are very deep. Similar observation of fibrous microstructure as observed for coatings deposited at 60°C is seen at a magnification of 1000x and covers almost the entire surface morphology of the coating. SEM images were taken on predominantly observed microstructures on the surface of coatings which is depicted in Figure 4.21 and Figure 4.22. Higher magnification of 3000x in Figure 4.21 and Figure 4.22 reveals a highly porous fibrous grain structure. EDX analysis shown in Figure 4.23 on the highly porous fibrous microstructure revealed a high percentage of iron element (metal substrate) and nickel with no zinc present as observed in first (a) and second (b) part of the spectrum in Figure 4.23 and hence through EDX analysis, the highly porous fibrous grain structure observed can be related to the microstructure of nickel. The high presence of iron in the EDX spectrum explains the high level of porosity (dark spots) in the fibrous structure of the grain which exposes the metal substrate.

EDX spectrum were obtained from targeted several points on the morphology obtained from the SEM and the spectrum were analysed on the elemental composition present in the coatings. Figure 4.23 and Figure 4.24 shows the spectrum obtained from EDX analysis.

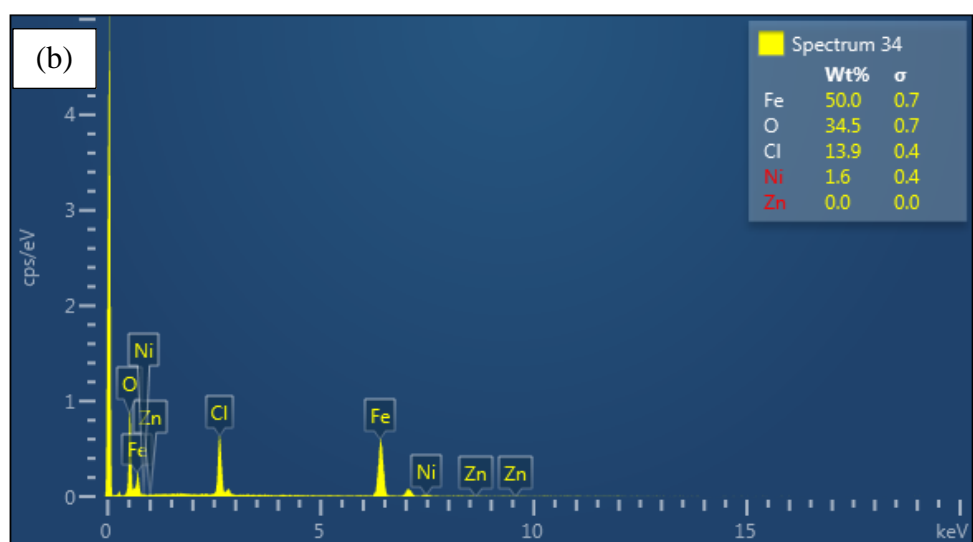
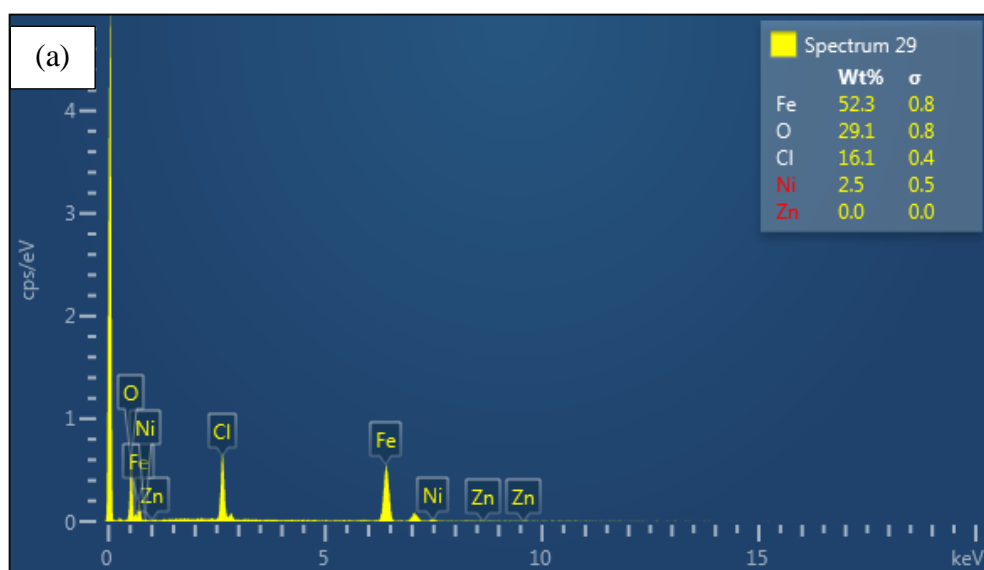


Figure 4.23: EDX Spectrum (a) and (b) for observed microstructure for zinc-nickel alloy coatings deposited at 70°C

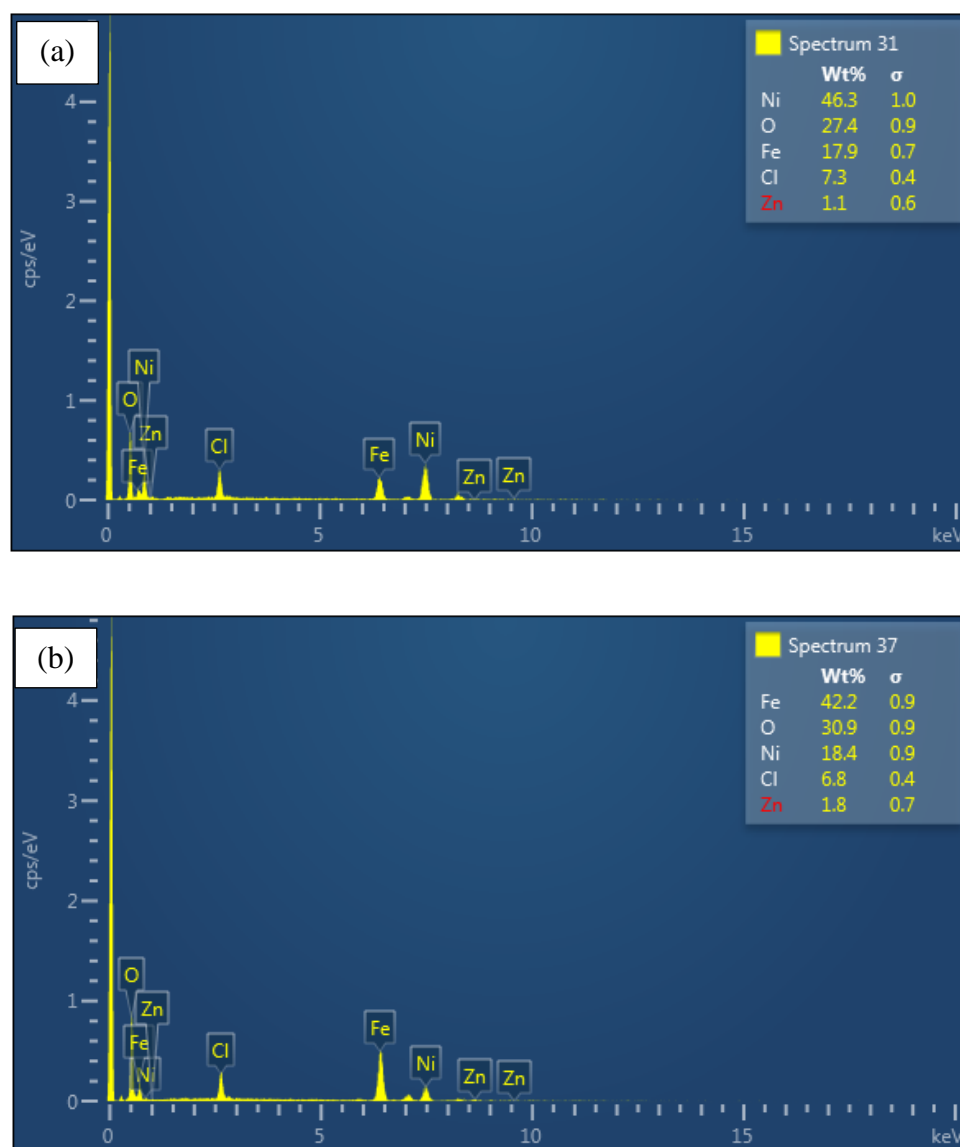


Figure 4.24: EDX Spectrum (a) and (b) for zinc-nickel alloy coatings deposited at 70°C

From the EDX spectrum data extracted from several points on the morphologies of the coatings, the average zinc-to nickel ratio weight percentage in the coatings at 70°C is observed to be 90 to 95% nickel and 5 to 10% zinc. Elements of oxygen, chlorine and iron are also present in the EDX spectrum.

Presence of chlorine in the coatings is related to the bath used for electrodeposition which mainly composed of chloride salts which facilitates the reduction of chloride ions to chlorine in the coatings. Oxygen diffusion in the coatings is related to the redox (oxidation-reduction) reaction during electrodeposition. Element of iron indicates the metal substrate and the difference in wt% of iron element obtained through EDX

analysis at different parts of the coatings deposited at different temperatures explains the uniformity of the coatings obtained. The non-uniformity increases with increasing deposition temperature.

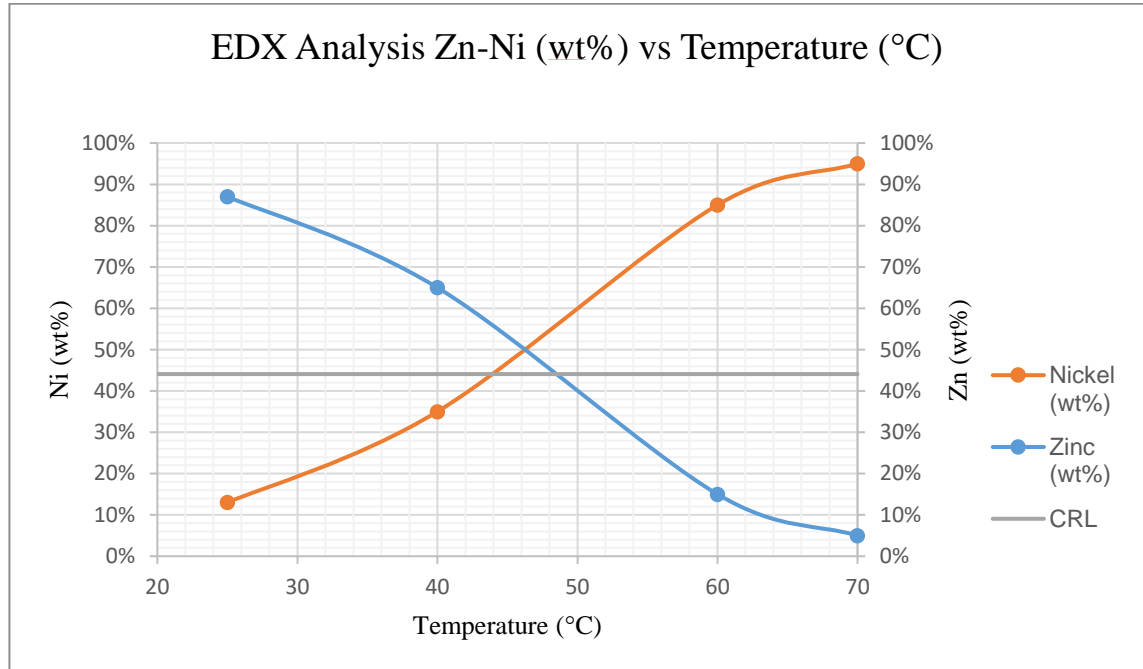


Figure 4.25: Zn-Ni content (wt%) vs Temperature (°C)

Figure 4.25 illustrates a summarized version of the EDX analysis results of the relationship between nickel and zinc content in the coatings with increasing deposition temperature.

It can be seen that the nickel content in the coatings rises with rise in temperature. CRL line calculated by Equation (3.1) differentiates between normal and anomalous type of deposition in the alloy deposition process that had occurred. CRL line is the representation of the concentration of nickel and zinc in the bath solution. At lower temperatures in the range value of 25°C to 40°C, it can be observed that the nickel content deposited in the coating is lower than the CRL line. This explains that at lower temperature range of 25°C to 40°C, anomalous alloy deposition is achieved which is the preferential deposition of less noble metal, zinc when compared to nickel and this is supported by the nickel content being below the CRL, lower than the nickel content in the bath solution. However, with larger increase in temperature in the range of 60°C to 70°C, nickel content in the coatings increases to 80 to 90% which results in transfer of alloy deposition from anomalous to normal type, a preferential deposition of the

more noble metal, nickel which is clearly depicted by the nickel wt% in the coating being above the CRL line, nickel wt% in the bath solution. Hence, deposition temperature plays an important role with increase in deposition temperature results in increase in nickel content which results in the shift from anomalous to normal deposition. LPR corrosion rate measurements were taken to investigate the effect of these microstructural and compositional change towards the corrosion resistance of deposited zinc-nickel alloy coatings.

#### 4.1.4 LPR Measurement

This chapter illustrates on the measurement of corrosion rate of zinc-nickel alloy at different temperatures of 25°C, 40°C, 60°C and 70°C by immersing the coated samples in 3.5 wt% NaCl solution for 24 hour with each reading taken hourly. Corrosion rate of plain carbon steel is taken to compare and analyse the corrosion behaviour of coated samples vs. plain carbon steel.

Figure 4.26 depicts the corrosion rate measurements of the coated samples comparing them to the corrosion rate of uncoated plain carbon steel.

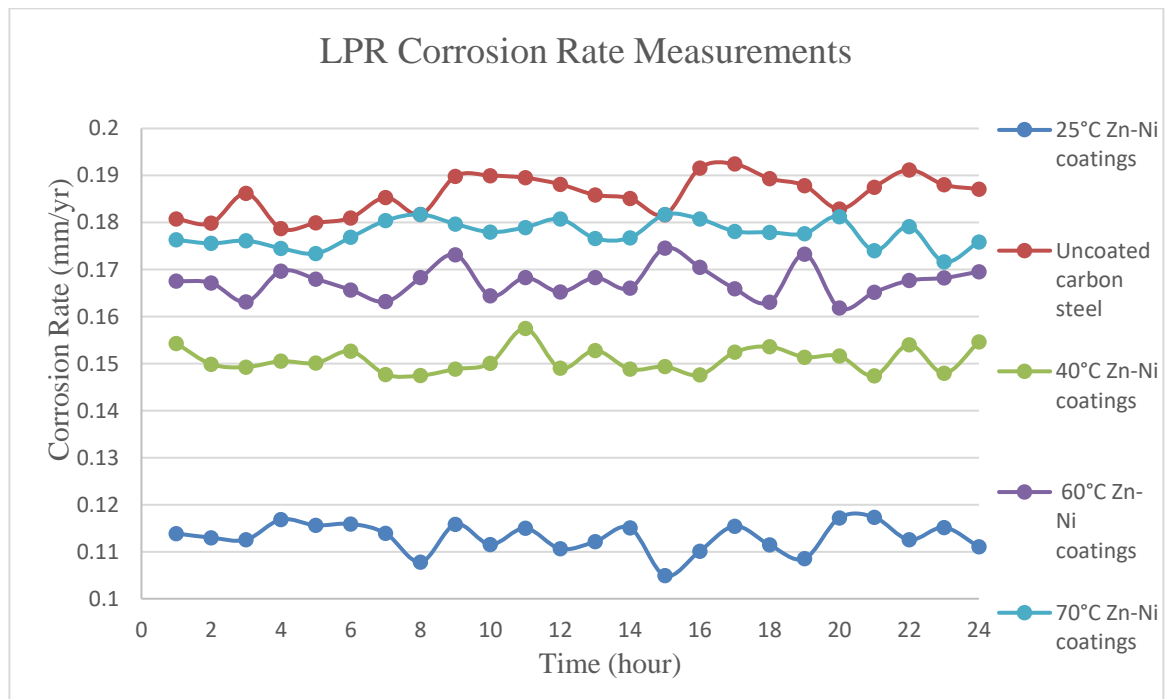


Figure 4.26: LPR corrosion rate measurements taken hourly for 24 hours



The average corrosion rate of the steel measured from the samples using LPR is presented in Table 4.1.

Table 4.1: Average corrosion rate of samples coated and uncoated obtained using LPR method

<b>Sample type</b>	<b>Average corrosion rate (mm/year)</b>
Uncoated carbon steel	0.19
25°C Zn-Ni coating	0.11
40°C Zn-Ni coating	0.15
60°C Zn-Ni coating	0.17
70°C Zn-Ni coating	0.18

As shown in Figure 4.26 and with the average corrosion rate obtained in Table 4.1, it can be observed that coated samples at 25°C, 40°C, 60°C and 70°C all provide good corrosion resistance when compared to uncoated carbon steel with lower corrosion rate measurements obtained than uncoated carbon steel. Comparing the corrosion rates of zinc-nickel alloy coated samples at different temperatures, zinc-nickel alloy coatings deposited at 25°C provide the highest corrosion resistance with lowest average corrosion rate obtained at 0.11 mm/year. This is followed by coatings deposited at 40°C with average corrosion rate of 0.15 mm/year. Observation from the trend in Figure 4.26 and average corrosion rate in Table 4.1 showed coatings deposited at elevated temperatures of 60°C and 70°C having higher corrosion rate of 0.17 mm/year and 0.18 mm/year slightly lower than uncoated carbon steel at 0.19 mm/year.

The highest corrosion resistance obtained of coating deposited at 25°C can be related to these primary factors of compactness, uniformity of coating, presence of micro-cracks and zinc-to-nickel content in the alloy. SEM and EDX observations from coatings deposited at 25°C reveals a (a) dense and compact morphology related to the observation of grain structure during SEM microstructural analysis in coatings deposited at 25°C (b) better uniformity of the coating at a lower temperature of 25°C when compared to higher temperature and (c) very low intensity of micro-cracks

present in the coatings at 25°C (d) ratio of zinc-to-nickel content in the ratio of Zn85%-Ni15% in the alloy.

Figure 4.27 and 4.28 illustrates the relationship between zinc and nickel content in the alloy with the average corrosion rate obtained from LPR.

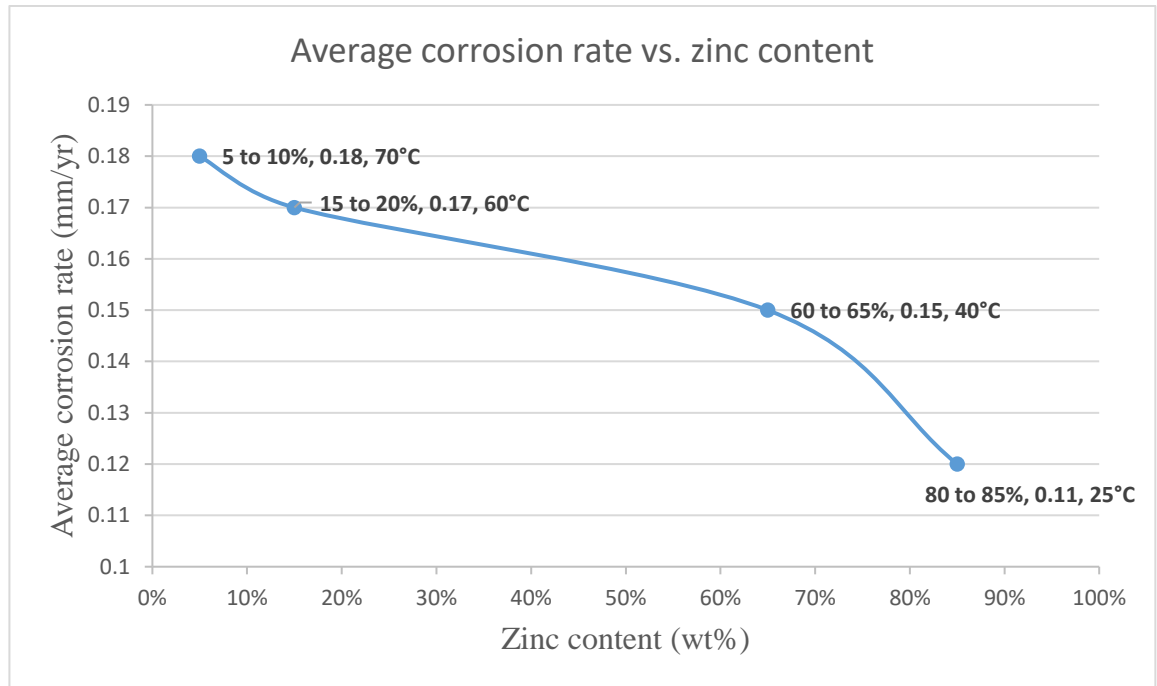


Figure 4.27: Average corrosion rate vs. zinc content

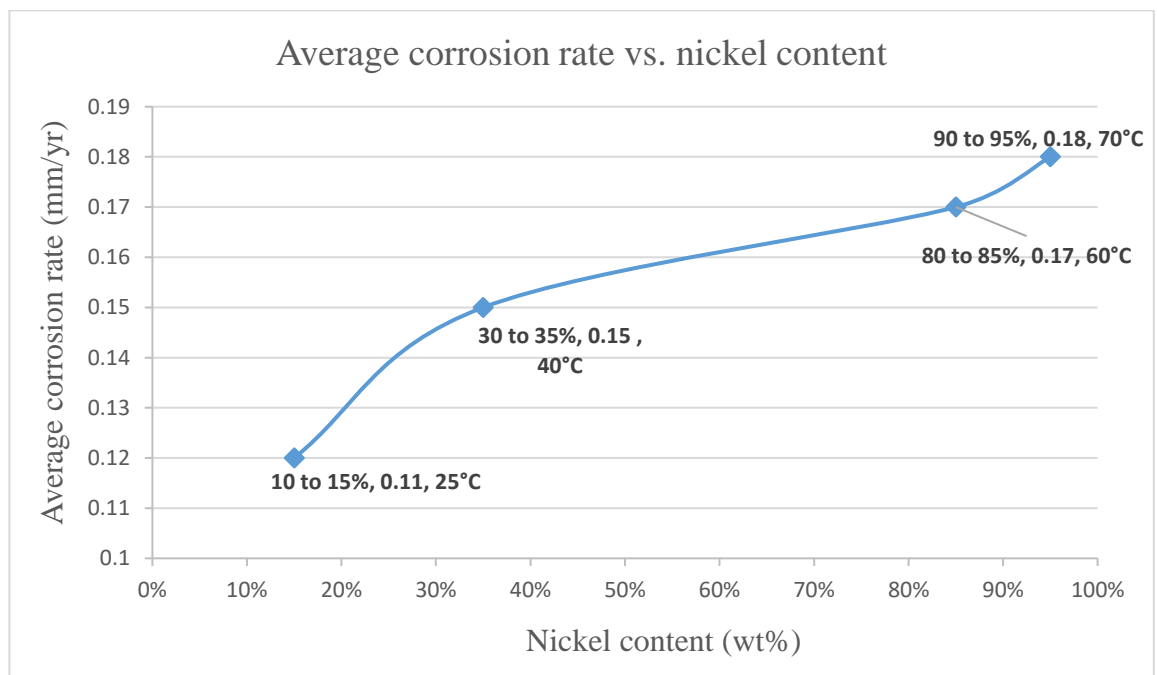


Figure 4.28: Average corrosion rate vs. nickel content

Nickel content in the alloy increases with increasing deposition temperature as observed through EDX analysis. Zinc-to-nickel ratio in the alloy has significant impact towards the corrosion resistance of zinc-nickel alloy. It can be seen from LPR measurements that alloy with Zn85%-Ni15%, the corrosion resistance is maximum.

As mentioned by [14-16, 18, 21], optimum corrosion resistance is achieved when the nickel content is in the value of 12% to 15% in the alloy. Zinc being a less noble metal, acts as an anode which dissolves or sacrifices in relation to nobler steel substrate under normal condition. Zinc is more preferred compared to a nobler metal such as nickel to be formed into coatings due to its high sacrificial property. However, the addition of nobler element into zinc is observed to have improved the corrosion resistance of zinc. With the addition of nickel element into zinc forming an alloy, the rate of zinc dissolving or sacrificing in relation to more nobler steel substrate is slower when compared to pure zinc alone. The more noble, nickel element functions to suppress or slows down the rate of zinc dissolution and this is only achieved in the optimum range of 12% to 15% as mentioned by the researches. This is because at this optimized range of nickel content, the zinc still retains its sacrificial function. However, when the nickel content in the coatings increases to more than 30%, the zinc's sacrificial function is lost and the alloy becomes more noble when compared to the steel substrate. At this point, the corrosion resistance of the alloy is purely based on the surface properties of the coatings.

Observations from SEM and EDX analysis on the surface morphology indicates compactness and uniformity decrease with increasing deposition temperature and increase in intensity of micro-cracks with increasing deposition temperature. The nickel content increases with deposition temperature (more than 30 wt% at 40°C and more than 80 wt% at 60°C and 70°C).

Alloy with nickel content of more than 30 wt% as in observed in coatings at 40°C, 60°C and 70°C loses its sacrificial function as a result the corrosion resistance of the alloy coatings is solely based on the surface properties of the coatings. However, with increasing temperature and nickel content in the alloy coatings as presented in Table 4.2, cracks intensity increases, coating uniformity and compactness decreases with temperature increase. This causes the corrosion rate to increase with increasing temperature as the nickel addition into zinc no longer improves the corrosion

resistance. The alloy becomes noble to metal substrate and the presence of cracks, decreased uniformity and compactness causes increase in the corrosion rate. The disruptions and cracks in the coatings accelerates the corrosion of the underlying metal substrate as the coating has now become nobler than the metal substrate. This concept explains the large difference in the corrosion rate measurement between coatings deposited 25°C and 40°C, 60°C and 70°C as shown in Figure 4.26.

Zinc-to-nickel ratio for coatings deposited at 25°C falls into the optimized range of nickel content of 12% to 15%, hence the sacrificial function of zinc is maintained in relation to addition of nickel element and this protects the metal substrate with increased corrosion resistance as zinc here acting as an anode is dissolved or sacrificed in relation to the metal substrate and with the addition of nickel within the value of 12% to 15% functions to slow down the rate of dissolution of zinc and this increases the corrosion resistance. The rate of dissolution of zinc decreases with the addition of nickel at the optimum value of 12% to 15% due to the potential increase of zinc-nickel alloy to a more positive value nearer to steel with the addition of nickel at 12% to 15% when compared to the potential of pure zinc at (-0.76 V) in the electrochemical series. This change in potential towards a more positive value narrows down the difference in the potential between steel at (-0.44 V) and zinc-nickel alloy. The potential of zinc-nickel alloy although increases to a positive value however is still lower than the potential of steel in the electrochemical series at the composition of 12% to 15%. This allows slower dissolution of zinc in the zinc-nickel alloy due to smaller difference in the potential series with the steel when compared to larger potential difference with steel for pure zinc. The higher anodic or active behavior of zinc is suppressed by the presence of nickel in the range of 12% to 15% where the anodic or active behavior of zinc is lowered down when compared to steel which allows slower dissolution of zinc which increases the corrosion resistance of zinc-nickel alloy providing corrosion protection for longer term when compared to pure zinc coatings which would corrode or dissolve at a faster rate. The disruptions and cracks in the coatings doesn't significantly affect the corrosion of metal substrate as the more anodic zinc would corrode preferentially.

The observation from microstructural and elemental compositional properties of the alloy correlates with results from LPR corrosion rate measurements with decreasing

corrosion resistance (higher rate of corrosion) with increasing deposition temperature and nickel content. The highest corrosion resistance obtained for coatings deposited at 25°C is related to the role of nickel in zinc-nickel alloy mainly and lower corrosion resistance at higher temperatures of 40°C, 60°C and 70°C is related to the surface or barrier properties such as uniformity, compactness and cracks in the alloy.

Table 4.2 simplifies the relationship between deposition temperature and the surface morphology, elemental composition and the corrosion resistance of zinc-nickel alloy coatings.

Table 4.2: Relationship between deposition temperature and variation in properties of zinc-nickel alloy coatings obtained

<b>Temperature</b>	<b>Surface Morphology</b>	<b>Nickel content (wt%)</b>	<b>Corrosion rate (mm/yr)</b>	<b>Corrosion resistance</b>
25°C	1. Dense and compact. 2. Higher uniformity. 3. Less micro-cracks.	10-15%	0.11	HIGHEST
40°C	1. Compactness decrease. 2. Uniformity less than 25°C. 3. Micro-cracks intensity increase.	30-35%	0.15	FAIR
60°C	1. Compactness less than 40°C. 2. Uniformity less than 40°C. 3. Micro-cracks intensity increase.	80-85%	0.17	NEARER TO CARBON STEEL
70°C	1. Highly porous. 2. Uniformity less than 60°C. 3. Micro-cracks intensity at highest.	90-95%	0.18	NEARER TO CARBON STEEL

Figure 4.29 shows the images of zinc-nickel alloy coatings at different temperatures after 24 hours of immersion in 3.5 wt% NaCl solution.

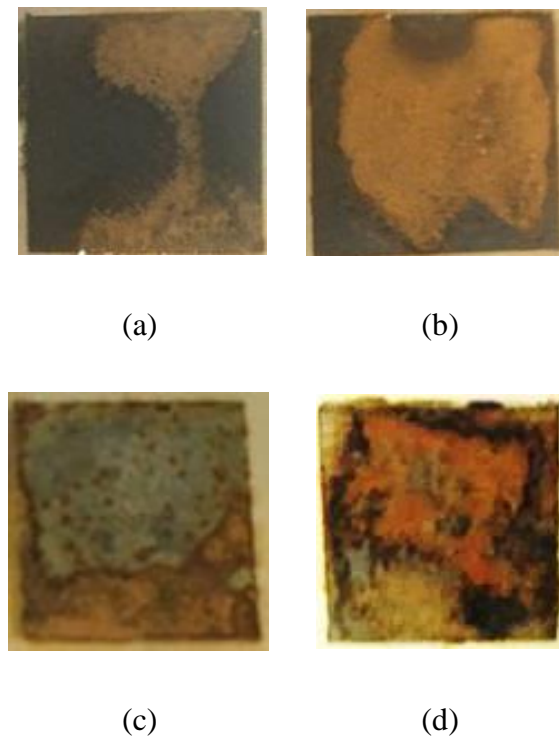


Figure 4.29: Observations on the coatings (a) 25°C (b) 40°C (c) 60°C and (d) 70°C after 24 hours immersion in 3.5 wt% NaCl solution

Observations as in Figure 4.29 shows the corrosion covers the least surface area for coatings deposited at 25°C. The severity of corrosion on the coatings increases with increasing temperature of 40°C, 60°C and 70°C with larger corroded surface area of the sample. This corrosion severity observed in terms of surface area correlates with LPR corrosion rate measurements with increasing corrosion rates with rise in deposition temperature.

## **CHAPTER 5: CONCLUSION AND RECOMMENDATION**

### **5.1 CONCLUSION**

Deposition parameters play a significant role in the process of electrodeposition which determines the properties of the coatings deposited. The influence of deposition temperature on the corrosion resistance of the zinc-nickel alloy coatings had been studied experimentally. Based on the findings from the study,

- a) Selection of optimized deposition parameters was done through literature review study.
- b) Electrodeposition of zinc-nickel alloy coatings was done by varying the deposition temperature parameter, maintaining other deposition parameter at optimized value.
- c) Micro-cracks are observed in all coatings with the crack intensity increasing with increasing temperature.
- d) The micro-cracks formation is attributed to internal stress which may be related to hydrogen evolution reaction of hydrogen diffusion inside coatings causing material brittleness inducing crack.
- e) Compactness and uniformity of coating decreases with increase in deposition temperature with coatings deposited at 25°C having dense and compact morphology.
- f) EDX analysis reveals the nickel content in the coating increasing with increasing deposition temperature.
- g) LPR corrosion rate measurement shows good corrosion resistance of all zinc-nickel coated samples deposited at different temperatures when compared to uncoated carbon steel.
- h) Zinc-nickel coated sample at 25°C shows the highest corrosion resistance when compared to samples coated at 40°C, 60°C and 70°C. This is related to the compactness, uniformity and less micro-cracks observed using SEM and zinc-to-nickel ratio content in the range of 10% to 15% nickel content as observed in EDX analysis. The corrosion rate measurements correlates with the findings from previous researches who mentioned on the highest corrosion resistance

achieved for zinc-nickel alloy with nickel content between 12% to 15%. The alloy maintains its sacrificial behaviour with respect to steel substrate within this composition whereas alloy with higher percentage of nickel becomes more noble than the steel substrate losing its sacrificial property accelerating the corrosion of the underlying less noble steel through areas of disruptions or cracks in the coatings which is observed in current study of decreasing corrosion resistance with increasing nickel content in the zinc-nickel alloy coatings.

- i) The lower corrosion rate of coatings deposited at 25°C is mainly related to the role of nickel in zinc-nickel alloy and higher corrosion rate at higher temperatures of 40°C, 60°C and 70°C is related to the lower barrier properties such as uniformity, compactness and cracks in the alloy.
- j) Zinc-nickel alloy coatings with the highest corrosion resistance, within required composition of 12% to 15%, dense and compact morphology, better uniformity with less crack is achieved with coatings deposited at 25°C.

## **5.2 RECOMMENDATION**

Current study involving zinc-nickel alloy coatings provides better understanding on the role of deposition parameters on the electrodeposition process to obtain high corrosion resistant and quality zinc-nickel alloy coatings.

Extension and optimization of the objectives of this paper can be done by investigating the influence of each deposition parameters consisting of bath composition, bath pH, current density and deposition potential involved in the electrodeposition process experimentally for better optimization of these parameters correlating them with the results obtained from current study on the deposition temperature for better understanding on the role of each deposition parameters on their effect on the electrodeposition, surface morphology characteristics, nickel content and corrosion resistance properties of zinc-nickel alloy.

The investigation of deposition parameters should also be done using different bath solution other than the chloride bath solution currently employed in this study. Other types of acidic bath such as that of acetate and sulfate and also alkaline baths have different chemical properties and this could have significant impact on the quality,



uniformity, surface and microstructural properties of the zinc-nickel alloy deposit obtained [8]. These change of deposit properties resulting from the usage of different bath can be studied to investigate its effect on the corrosion resistance properties of the zinc-nickel alloy.

Improvement and enhancement in zinc-nickel alloy coatings through these recommendations is required to further enhance the current study to allow better optimization of the electrodeposition process to obtain quality zinc-nickel alloy coatings of the highest corrosion resistance which is required in various industrial applications involving the use of carbon steel especially in the automotive and aerospace industries.

## REFERENCES

- [1] M. M. Abou-Krishna, "Influence of Ni  $2+$  concentration and deposition potential on the characterization of thin electrodeposited Zn–Ni–Co coatings," *Materials Chemistry and Physics*, vol. 125, pp. 621-627, 2011.
- [2] H. Durmuş, "Mechanical properties and corrosion behaviour of MIG welded 5083 aluminium alloy," *Materials Testing*, vol. 53, pp. 356-363, 2011.
- [3] M. Gavrilă, J. Millet, H. Mazille, D. Marchandise, and J. Cuntz, "Corrosion behaviour of zinc–nickel coatings, electrodeposited on steel," *Surface and coatings technology*, vol. 123, pp. 164-172, 2000.
- [4] M. H. Seo, D. J. Kim, and J. S. Kim, "The effects of pH and temperature on Ni–Fe–P alloy electrodeposition from a sulfamate bath and the material properties of the deposits," *Thin Solid Films*, vol. 489, pp. 122-129, 2005.
- [5] K. S. Lew, M. Raja, S. Thanikaikarasan, T. Kim, Y. D. Kim, and T. Mahalingam, "Effect of pH and current density in electrodeposited Co–Ni–P alloy thin films," *Materials Chemistry and Physics*, vol. 112, pp. 249-253, 2008.
- [6] M. Farzaneh, K. Raeissi, and M. Golozar, "Effect of current density on deposition process and properties of nanocrystalline Ni–Co–W alloy coatings," *Journal of Alloys and Compounds*, vol. 489, pp. 488-492, 2010.
- [7] F. Elkhatabi, M. Benballa, M. Sarret, and C. Müller, "Dependence of coating characteristics on deposition potential for electrodeposited Zn–Ni alloys," *Electrochimica acta*, vol. 44, pp. 1645-1653, 1999.
- [8] Y. D. Gamburg and G. Zangari, *Theory and practice of metal electrodeposition*: Springer Science & Business Media, 2011.

- [9] O. Hammami, L. Dhouibi, and E. Triki, "Influence of Zn–Ni alloy electrodeposition techniques on the coating corrosion behaviour in chloride solution," *Surface and Coatings Technology*, vol. 203, pp. 2863-2870, 2009.
- [10] H. Nakano, M. Matsuno, S. Oue, M. Yano, S. Kobayashi, and H. Fukushima, "Mechanism of anomalous type electrodeposition of Fe-Ni alloys from sulfate solutions," *Materials transactions*, vol. 45, pp. 3130-3135, 2004.
- [11] G. Roventi, R. Fratesi, R. Della Guardia, and G. Barucca, "Normal and anomalous codeposition of Zn–Ni alloys from chloride bath," *Journal of applied electrochemistry*, vol. 30, pp. 173-179, 2000.
- [12] G. Barcelo, M. Sarret, C. Müller, and J. Pregonas, "Corrosion resistance and mechanical properties of zinc electrocoatings," *Electrochimica Acta*, vol. 43, pp. 13-20, 1998.
- [13] C. Bowden and A. Matthews, "A study of the corrosion properties of PVD Zn-Ni coatings," *Surface and Coatings Technology*, vol. 76, pp. 508-515, 1995.
- [14] A. Conde, M. Arenas, and J. De Damborenea, "Electrodeposition of Zn–Ni coatings as Cd replacement for corrosion protection of high strength steel," *Corrosion Science*, vol. 53, pp. 1489-1497, 2011.
- [15] Z.-f. Lin, X.-b. Li, and L.-k. Xu, "Electrodeposition and corrosion behavior of zinc–nickel films obtained from acid solutions: effects of TEOS as additive," *Int. J. Electrochem. Sci*, vol. 7, pp. 12507-12517, 2012.
- [16] K. Baldwin, M. Robinson, and C. Smith, "The corrosion resistance of electrodeposited zinc-nickel alloy coatings," *Corrosion science*, vol. 35, pp. 1267-1272, 1993.
- [17] K. Baldwin, M. Robinson, and C. Smith, "Corrosion rate measurements of electrodeposited zinc-nickel alloy coatings," *Corrosion science*, vol. 36, pp. 1115-1131, 1994.

- [18] A. El Hajjami, M. Gigandet, M. De Petris-Wery, J. Catonne, J. Duprat, L. Thiery, *et al.*, "Characterization of thin Zn–Ni alloy coatings electrodeposited on low carbon steel," *Applied Surface Science*, vol. 254, pp. 480-489, 2007.
- [19] R. Gnanamuthu, S. Mohan, G. Saravanan, and C. W. Lee, "Comparative study on structure, corrosion and hardness of Zn–Ni alloy deposition on AISI 347 steel aircraft material," *Journal of Alloys and Compounds*, vol. 513, pp. 449-454, 2012.
- [20] M. Kwon, D.-h. Jo, S. H. Cho, H. T. Kim, J.-T. Park, and J. M. Park, "Characterization of the influence of Ni content on the corrosion resistance of electrodeposited Zn–Ni alloy coatings," *Surface and Coatings Technology*, vol. 288, pp. 163-170, 2016.
- [21] T. Byk, T. Gaevskaya, and L. Tsybulskaya, "Effect of electrodeposition conditions on the composition, microstructure, and corrosion resistance of Zn–Ni alloy coatings," *Surface and Coatings Technology*, vol. 202, pp. 5817-5823, 2008.
- [22] M. M. Abou-Krishna, M. I. Attia, F. H. Assaf, and A. A. Eissa, "Influence of pH on the Composition, Morphology and Corrosion Resistance of Zn-Ni-Mn Alloy Films Synthesized by Electrodeposition," *Int. J. Electrochem. Sci*, vol. 10, pp. 2972-2987, 2015.
- [23] E. Levy and R. MacInnis, "Effect of pH on structure and mechanical properties of electrodeposited iron," *Journal of Chemical Technology and Biotechnology*, vol. 18, pp. 281-284, 1968.
- [24] S. A. El Rehim, E. Fouad, S. A. El Wahab, and H. H. Hassan, "Electroplating of zinc-nickel binary alloys from acetate baths," *Electrochimica acta*, vol. 41, pp. 1413-1418, 1996.
- [25] R. Albalat, E. Gomez, C. Müller, M. Sarret, E. Valles, and J. Pregonas, "Electrodeposition of zinc-nickel alloy coatings: influence of a phenolic derivative," *Journal of Applied Electrochemistry*, vol. 20, pp. 635-639, 1990.

- [26] H. Atapattu, D. De Silva, K. Pathiratne, and I. Dharmadasa, "Effect of stirring rate of electrolyte on properties of electrodeposited CdS layers," *Journal of Materials Science: Materials in Electronics*, vol. 27, pp. 5415-5421, 2016.
- [27] S. Ghaziof and W. Gao, "Electrodeposition of single gamma phased Zn–Ni alloy coatings from additive-free acidic bath," *Applied Surface Science*, vol. 311, pp. 635-642, 2014.
- [28] S. Yogesha, K. U. Bhat, and A. C. Hegde, "Effect of Current Density on Deposit Characters of Zn-Co Alloy and their Corrosion Behaviors," *Synthesis and Reactivity in Inorganic, Metal-Organic, and Nano-Metal Chemistry*, vol. 41, pp. 405-411, 2011.
- [29] H. Ashassi-Sorkhabi, A. Hagrah, N. Parvini-Ahmadi, and J. Manzoori, "Zinc–nickel alloy coatings electrodeposited from a chloride bath using direct and pulse current," *Surface and Coatings Technology*, vol. 140, pp. 278-283, 2001.
- [30] X. Qiao, H. Li, W. Zhao, and D. Li, "Effects of deposition temperature on electrodeposition of zinc–nickel alloy coatings," *Electrochimica Acta*, vol. 89, pp. 771-777, 2013.
- [31] G. A. Ali, M. M. Yusoff, Y. H. Ng, H. N. Lim, and K. F. Chong, "Potentiostatic and galvanostatic electrodeposition of manganese oxide for supercapacitor application: A comparison study," *Current Applied Physics*, vol. 15, pp. 1143-1147, 2015.
- [32] S. Pyun, Lee, *Electrochemistry of Insertion Materials for Hydrogen and Lithium* vol. Springer Science & Business Media: Springer 2012.
- [33] A. W. Bott, "Controlled Current Techniques," *epsilon*, vol. 47906, p. 1382.
- [34] A. Velichenko, M. Sarret, and C. Müller, "Nature of the passive film formed at a zinc anode in zinc–nickel containing solutions," *Journal of Electroanalytical Chemistry*, vol. 448, pp. 1-3, 1998.

- [35] A. Alfantazi, G. Brehaut, and U. Erb, "The effects of substrate material on the microstructure of pulse-plated Zn–Ni alloys," *Surface and Coatings Technology*, vol. 89, pp. 239-244, 1997.

## APPENDICES

### CORROSION RATE (CR) AND COMPOSITION REFERENCE LINE (CRL) CALCULATION

#### 1. Composition Reference Line (CRL)

$$CRL = \frac{c(Ni^{2+})}{c(Ni^{2+} + Zn^{2+})}$$

$$c(Ni/Zn^{2+}) = \frac{\text{Amount of salt in bath solution (g/L)}}{\text{Molar mass of salt (g/mol)}}$$

$$c(Ni^{2+}) = \frac{110 \text{ g/l}}{237.69108 \text{ g/mol}}$$

$$c(Ni^{2+}) = 0.46278 \text{ mol/L}$$

$$c(Zn^{2+}) = \frac{88 \text{ g/l}}{136.286 \text{ g/mol}}$$

$$c(Zn^{2+}) = 0.587 \text{ mol/L}$$

$$CRL = \frac{0.46278 \frac{\text{mol}}{\text{L}}}{0.46278 \frac{\text{mol}}{\text{L}} + 0.587 \frac{\text{mol}}{\text{L}}}$$

$$CRL = 0.4408 = 44.08\%$$

## 2. Corrosion rate (CR) calculation

Corrosion current ( $i_{\text{corr}}$ ),

$$i_{\text{corr}} = \frac{B}{R_p}$$

$$i_{\text{corr}} = \frac{26 \text{ mV}}{R_p (\Omega \text{ cm}^2)} = \frac{26 \times 10^{-3} \text{ V}}{R_p (\Omega \text{ cm}^2)} = \frac{26000 \text{ } \mu\text{A}}{R_p \text{ cm}^2}$$

Corrosion rate (CR),

$$\text{Corrosion Rate} = K \cdot EW \cdot \frac{i_{\text{corr}}}{\rho \cdot A} \text{ (mm/yr)}$$

$K$  = constant that defines the unit for corrosion rate =  $3.27 \times 10^3 \frac{\text{mm} \cdot \text{g}}{\mu\text{A} \cdot \text{cm} \cdot \text{yr}}$

$EW$  = Equivalent weight of the steel (X52 carbon steel) = 27.92

$\rho$  = Density of the X52 carbon steel =  $7.86 \frac{\text{g}}{\text{cm}^3}$

$A$  = Exposed Surface area of the X52 carbon steel =  $1 \text{ cm} \times 1 \text{ cm} = 1 \text{ cm}^2$

$$\text{CR} = 3.27 \times 10^3 \frac{\text{mm} \cdot \text{g}}{\mu\text{A} \cdot \text{cm} \cdot \text{yr}} \cdot (27.92) \cdot \frac{i_{\text{corr}} \frac{\mu\text{A}}{\text{cm}^2}}{7.86 \cdot (1 \text{ cm}^2) \frac{\text{g}}{\text{cm}^3}}$$

$$\text{Corrosion Rate} = 0.01162 \cdot i_{\text{corr}} \text{ (mm/yr)}$$

Substituting  $i_{\text{corr}}$  equation into CR equation,

$$\text{Corrosion Rate (CR)} = 0.1162 \cdot \frac{26000}{R_p} \text{ (mm/yr)}$$



$$\text{Corrosion Rate (CR) of X52 carbon steel} = \frac{302.12}{R_p} \text{ (mm/yr)}$$